scientific reports

Check for updates

OPEN

Optimal allocation of distributed energy resources to cater the stochastic E-vehicle loading and natural disruption in low voltage distribution grid

Devender Kumar Saini[1]✉, Monika Yadav[1]✉ & Nitai Pal[2]

The everyday extreme uncertainties become the new normal for our world. Critical infrastructures like electrical power grid and transportation systems are in dire need of adaptability to dynamic changes. Moreover, stringent policies and strategies towards zero carbon emission require the heavy influx of renewable energy sources (RES) and adoption of electric transportation systems. In addition, the world has seen an increased frequency of extreme natural disasters. These events adversely impact the electrical grid, specifically the less hardened distribution grid. Hence, a resilient electrical network is the demand of the future to fulfill critical loads and charging of emergency electrical vehicles (EV). Therefore, this paper proposes a two-dimensional methodology in planning and operational phase for a resilient electric distribution grid. Initially stochastic modelling of EV load has been performed duly considering the geographical feature and commute pattern to form probability distribution functions. Thenceforth, the impact assessment of extreme natural events like earthquakes using damage state classification has been done to model the impact on distribution grid. The efficacy of the proposed methodology has been tested by simulating an urban Indian distribution grid with mapped EV on DigSILENT PowerFactory integrated with supervised learning tools on Python. Subsequently 24-h load profile before event and after event have been compared to analyze the impact.

Keywords Electrical distribution grid, Resiliency, Renewable energy sources, Natural disaster, Electric vehicle load

List of symbols

Indices and sets

$\sqcap$	Load failure probability estimator
σ	Standard deviation
ϕ	Load failure frequency estimator
μ	Mean value

Abbreviations

COP	Conference of the parties
DG	Distributed generations
ES	Energy storage
EPNS	Expected power not served
EV	Electric vehicle
LOLF	Loss of load frequency
LOLP	Loss of load probability
LVRT	Low voltage ride through

[1]Electrical Cluster, School of Engineering, University of Petroleum & Energy Studies, Dehradun, India. [2]Department of Electrical Engineering, Indian Institute of Technology (Indian School of Mines), Dhanbad, India. ✉email: dev.iit.roorkee@gmail.com; dksaini@ddn.upes.ac.in; Monika.yadav022@gmail.com

MG	Micro grid
$P_{charger}$	Power rating of the charger
PDF_{Ar}	Probability distribution function of arrival time
PDF_{Dr}	Probability distribution function of departure time
PGA	Peak ground acceleration
PSO	Particle swarm optimization
RES	Renewable energy sources
SHO	Spotted hyena optimizer
SLD	Single line diagram
SOC	State of charge
$T_{charing}$	Charging time

Contemporarily a green planet is the foremost policy for most countries like G7, G10, G15 etc. Besides, the Paris agreement of COP21 has been accepted by 192 countries so far. This necessitates the maximum reliance on renewable energy sources (RES) and adoptions of electric vehicles (EVs) by developed and developing countries. However, the integration of RES with controlling devices substantiate the entire grid system to follow the grid codes provided by operators of the state/country[1]. In addition, the dynamically changing definition of smart grid, comprises EVs, energy storage (ES), formation of micro grids (MGs), communication protocols etc., restructure the conventional grid as shown in Fig. 1.

The heavy penetration of RES in conventional electrical grid undoubtedly improves the flexibility of grid but reduces the reliability and safety due to intermittent nature of it[3]. Even the inclusion of RES plays a vital role in reaching the sustainable goals. Moreover, the world has seen an increased frequency of extreme natural disasters. These events adversely impact the electrical grid, specifically the less hardened distribution grid. Therefore, it is imperative to analyze the critical infrastructures like electrical power grid under extreme events like natural disaster and cyber-attack possibilities. However, it is evident from the literature that optimal uses of distributed generations (DGs) can minimize the overall impact on a power system network due to extreme events. Consequently, this paper explores the DGs operation, modelling & analyzing of EV load and impact of earthquake on overall distribution grid resiliency.

Relevance of DGs in distribution grid

The distribution system was initially built to cater the different load consumers without any local electrical generation. In contrast, presently, distribution companies rely on DGs for several benefits. Despite the clear advantages of integration RES-DGs, it presents technical challenges in terms of voltage, frequency, phase unbalance, short circuit level and protection coordination. Eventually, integrating RES-DGs improves the flexibility to cater surplus demand, but the price must be made in terms of system stability. Moreover, there are certain advantages of DGs integration apart from matching demand response. Like, author in Ref.[4], presents a method which suppresses the ferro-resonance issue with the DG on the IEEE 33 bus system. In addition, in paper[5], the author presented the impact of low voltage ride through (LVRT) during the sudden disconnection of large RES plant.

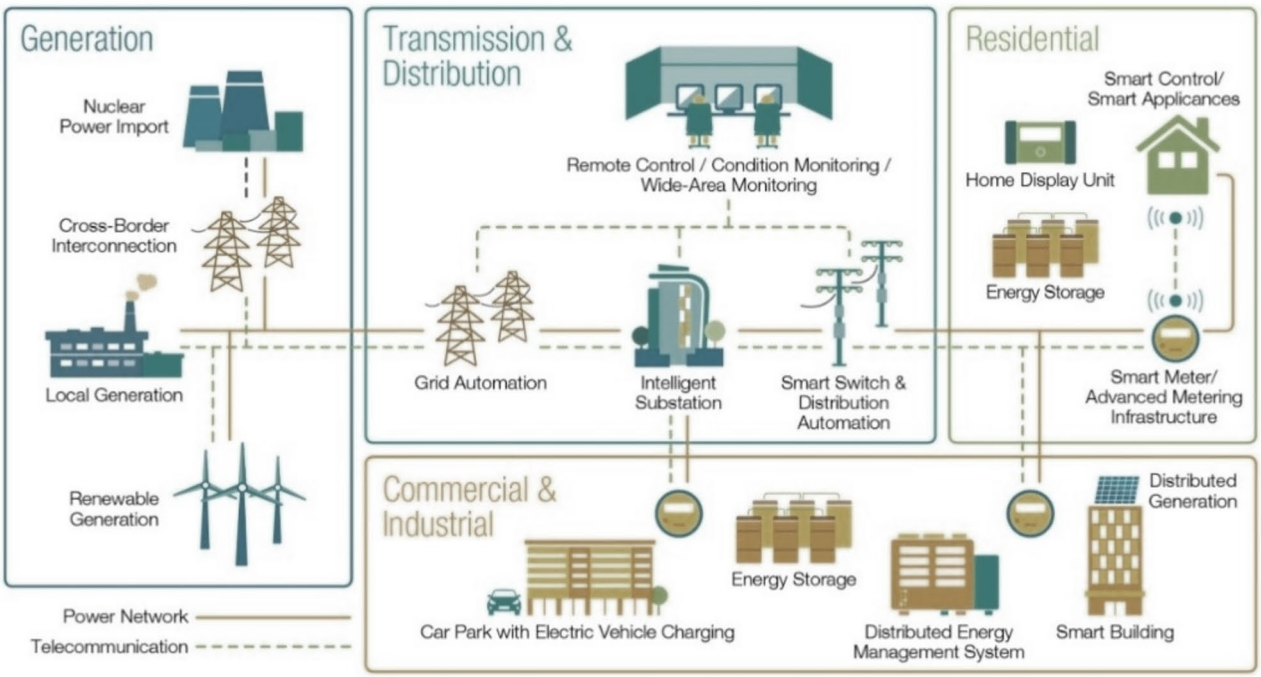

Figure 1. Contemporary smart grid[2].

Furthermore, the author also presented various control strategies for controlling the effect of LVRT. However, it is concluded that the intermittent nature of RES-DGs can also lead towards mismatch in generation and demand.

Stochastic loading of EVs

EVs are revolutionary technology of this century, meant to achieve a green environment. In contrast, EVs are seen as stochastic load on distribution grid. It is evident from the literature that the DGs placement improves the voltage profile and minimizes power losses. Conversely, EV load in distribution grid can degrade the voltage profile, power quality and may enhance the power losses, if their future growth with their load profile and pattern is not being considered in planning stage. In this regard, the maximum stress will be on the low voltage distribution grid, as 90% of personnel vehicles are probably charged at home charging stations, whereas the remaining 10% are on commercial charging facilities[6]. Moreover, the penetration of EVs will be increased exponentially in the future. For an example, the capital city of India, Delhi has worst air quality index. Therefore, EVs will be adopted more rapidly than other metro cities in India. On that note, a report prepared by A. Sharma[6], presents the load profile of Delhi, with and without EVs for 2025 and 2030, as shown in Figs. 2 and 3, respectively. In addition, the report graph shows that there is an additional approximate 2 GW/day increase in the load due to EVs by the year 2025 and 8 GW by 2030.

Therefore, it is imperative to study the dynamic loading of EVs over electric distribution grid. Consequently,, recent literature presents the many modelling techniques to calculate the EV load demand over distribution grid. However, many of these modelling techniques considered controlled charging behavior which subsequently imposes wrong EV demand over 24 h of period. Moreover, few recent studies suggested the strategies for sustainable deployment of EV infrastructure without considering the RES integration and its intermittency[7]. In Ref.[7], authors have considered only power quality issue of the grid to develop the sustainable strategies for EV infrastructure deployment. However, without considering the future aspect of grid dynamics, it is absurd to say that any strategy would be sustainable towards EV infrastructure development. Furthermore, in Ref.[8], authors have presented the optimal allocation of RES and DGs and validated the results on 28 bus Indian distribution system. The presented paper[8], shows the impact of renewable DGs and EVs on distribution grid. However, the paper limits its finding in terms of EV demand modelling and quasi dynamic load flow solution. Moreover, the

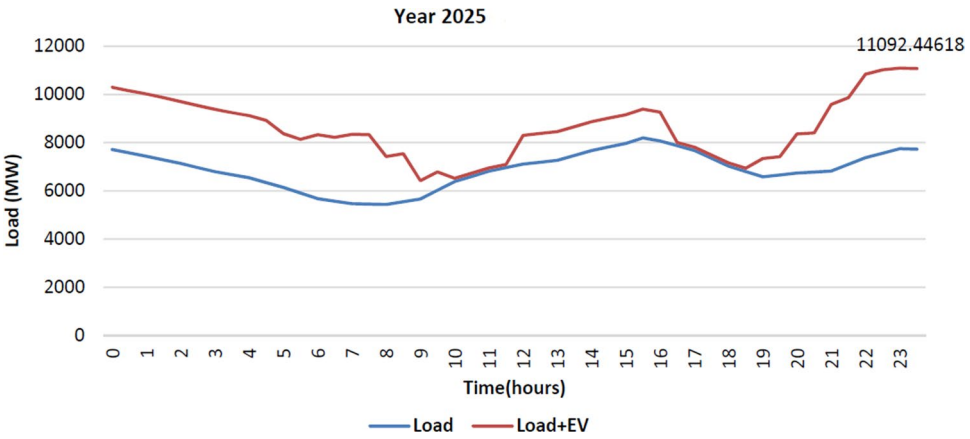

Figure 2. Delhi (India) load profile with and without EV for 2025[6].

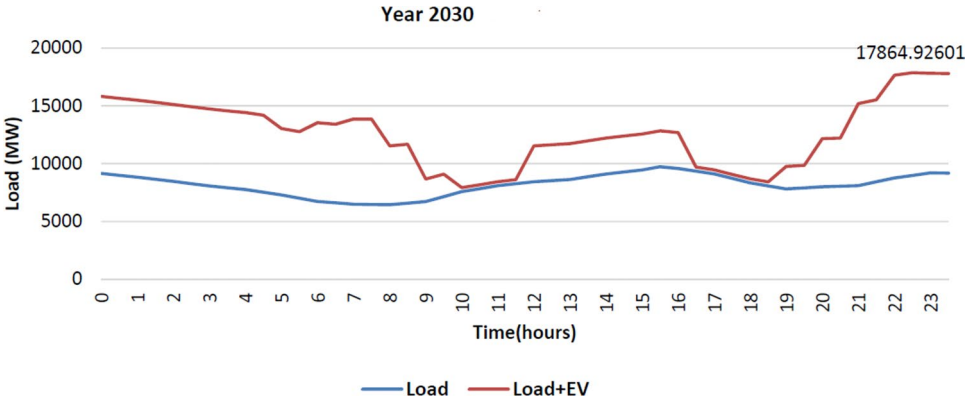

Figure 3. Delhi (India) load profile with and without EV for 2030[6].

paper does not include the EV driving behavior to formulate the 24-h load demand and, also lacks in terms of RES intermittency. Similarly, the paper[9], presents a method to minimize the EV charging impact in distribution grid using DGs and DSTATCOM. However, while modelling the EV load, the author considered the EV load as constant and performed the load flow on absolute value.

Therefore, this presented manuscript caters such aspect by presenting an idea, on dynamically changing grid conditions in terms of EV load uncertainty and RES intermittency. However, the unavailability of data on growth rate, charging pattern, social behavior and driving range of different categories of EVs (like, personal, utility vehicle, city commute, big transportation trucks), necessitate the use of probability theory to model the EVs loading as random variable. Therefore, it becomes necessary to model the EVs stochastic pattern while planning for RES-DGs integration. Consequently, the problem statement has two variables, intermittent generation (RES) and partly load (EVs), which need to be taken care of by planning engineers duly accounting for the future uncertainty.

Impact of natural disasters on electric grid

Recently, the world has seen many catastrophic events like earthquakes, cyclones, floods, cloudbursts, etc. These events adversely impact the electrical grid, as shown in Fig. 4, and the recent disaster and their impact on electrical infrastructure are mentioned in Table 1[10–14]. Also, the map in Table 1 is showing the storm's track and intensity, as per the Saffir–Simpson scale[15–19]. The disruption of electrical infrastructure halts all the essential and non-essential supply. The critical essential utilities like water supply, communication, fire utility and critical community center loads require reliable electrical power to cope with the post-disaster situation and to reinforce the recovery process[20]. Therefore, a resilient distribution grid is a prima requirement, serving at least critical utilities and essential services. Recent literature has fair amount of studies, addressing the power grid resiliency. For an example, a dart game theory approach for the enhancement of resiliency during extreme event is presented[21]. In addition, the proposed model also reduces load shedding and cost of restoration.

Contribution of the presented paper

The transition towards green energy is going to be faster than ever. Consequently, the entire power system structure will see many reinforcements to adapt dynamic changes as discussed above. The maximum changes will occur on low (440 V) and medium voltage (up to 33 kV) distribution grid. The distribution part is also most vulnerable towards natural disruption. Therefore, a sustainable planning of distribution grid with modern machine learning tools is essential for utility. The paper provides a detailed analysis of voltage variations over a 24-h period with up to 30% EV penetration, highlighting the critical need for grid ancillary services to support frequency and reactive power.

Moreover, the presented study examines grid transformation during extreme events over a 24-h timeframe, underscoring the necessity for distributed generation (DG) allocation to ensure grid stability from seconds to minutes. This research offers a fresh perspective on power system planning, emphasizing the preparedness required for high EV penetration and the resilience needed against high-impact events.

The paper also advocates for the integration of DGs and battery storage to enhance power flow and grid stability. It also explores optimized battery charging and discharging strategies, contributing to the discourse

Figure 4. Damaged electrical infrastructure and solar plants after natural disaster[22].

Disruption/year	Wind gust (Km/h)	Map showing the storm's track and intensity, as per the Saffir–Simpson scale[15–19] (map images are directly taken from[15–19] without any modifications)	Total damage cost
Amphan (2020)	150		Approximated damage cost: $14 billion
Tauktae (2021)	195		Approximated damage cost: $2.1billion
Mocha (2023)	256		Approximated damage cost: $1.07 million
Sitrang (2022)	83		Approximated damage cost: $34.4 million
Jawad (2021)	75		Approximated damage cost: $50.35 million

Table 1. Recent natural disruption[10–14].

on improving grid efficiency and reliability. Overall, this work provides valuable insights and practical solutions for future power system planning and management in the context of increasing EV adoption and extreme event resilience. The novel contributions (objectively) of the presented paper are stated hereunder:

- RES-DGs sizing and siting to improve voltage profile and to reduce carbon emission duly accounting the intermittency of RES.
- Probabilistic approach to model EV load profile based on driving distance, battery status and time of charging and discharging.
- Optimal allocation of RES-DGs to minimize the adverse effect of EV load on voltage stability and power quality.
- Modelling of natural disaster for vulnerability assessment of distribution feeders.
- Application of supervised learning algorithm in planning phase for planning of resilient distribution grid against natural disruption.

The rest of the paper is organized into 6 sections. Section "Introduction" weaves the background of the problem statement and subsequently highlights the contribution of the paper. Section "Power system resiliency modelling" formulates the power system resiliency modelling. Section "Impact modelling of EV load on distribution grid" models the randomness of EV load on distribution grid using probabilistic approach in Indian context. Framework for sizing & siting of solar PV in distribution grid along with EV loading has been presented in section "Problem formulation for sizing and siting DGs". Section "Impact of extreme event on an urban Indian electric grid" deduces the impact analysis for an extreme disruption using machine learning techniques and an urban Indian electric grid of Dehradun city has been taken to examine the efficacy of framework. Lastly, the findings of the presented manuscript have been concluded in section "Conclusion".

Power system resiliency modelling

The electric grid has a significant role in human life; primarily things depend on electricity. Therefore, a resilient power system structure that can provide electricity supply during disastrous events (intentional/unintentional) is required. The traditional grids were constructed to satisfy the demand in usual operating condition. However, it is evident now that the conventional grid is highly vulnerable to high impact natural disruption. Therefore, it is time to improve the resiliency of the distribution network by restoring the power in the distribution system quickly after the event. It is apparent from the literature that DERs (specifically solar PV) along with optimally sized ES units (mostly battery storage) have proven to enhance the grid resiliency during the catastrophic events[23–27]. Moreover, the author[28], proposed a metric for finding the optimal location of energy storage units in the distribution system, further improving the voltage profile. In paper[29], optimal sizing and siting of the constant and variable capacitors during grid connection and isolated modes are identified using the spotted hyena optimizer (SHO) algorithm. Furthermore, the author includes various load levels, and the results show an overall net cost saving with DGs duly including the capability of active and reactive power injection. In addition, quantum annealing methodology is presented by Silva for minimizing the power loss in the network[30]. The power grid's reliability differs from the grid resiliency concept in terms of operating and time horizon. The subsequent sections present the details about power grid resilient network and how it differs from the reliability aspect.

Reliable electric grid

The main objective of an electrical grid is to deliver a reliable and continuous power supply. Hence, reliability in terms of the electrical grid deals with high-frequency low-impact events and considers the equipment's ageing effects. The system's reliability is its ability to continuously supply power to the loads without disruption[31]. The reliability of a power system is measured by various indices such as probability vs expectation in load loss, frequency and duration of power failure, and severity of the failure[32]. These indices are evaluated either empirically or predictively. In empirical methods, reliability indices are measured by data collection, while in predictive, many ways can be considered for the evaluation, such as network reconfiguration, system behavior, operational characteristics etc. The three main indices are as follows.

i. Loss of load probability estimation (LOLP):

$$LOLP = E[\sqcap], \tag{1}$$

where $\sqcap = \frac{1}{T}\sum_{i=1}^{N_{cy}} T_{i(d)}$ and $T = N_{cy}.T_{ry}$. $\sqcap$ = Load failure probability estimator; cy = cycle; E = Expectation operator; T = Time period. $N_{cy} = No.ofcyclesinsimulation$; $T_{i(d)}$ = Interruption duration.

ii. Loss of load frequency estimation (LOLF): It estimates the frequency of failures per unit of time.

$$LOLF = E[\Phi], \tag{2}$$

where Φ = Load failure frequency estimator and is given by $\Phi = \frac{N_{cy}}{T}$

iii. Expected power not served estimation (EPNS): This index evaluates the failure states of expected demand/power not served. The EPNS is given as:

$$EPNS = \sum_{f_i \epsilon F_i} P\{fi\}.L\{fi\}, \tag{3}$$

where $P\{fi\} = Probabilityofoccurrenceand L\{fi\} = loadcurtailmentstate$; $F_i = setoffailurestates$.

Furthermore, the power system reliability indices can be divided based on nature, either probabilistic or deterministic. The probabilistic index is much more challenging to incorporate as they deal with uncertainties like loss of power but provide a quality solution. In contrast, the deterministic index is a reserved type and easy to use. However, the reliability factor is incorporated in decision or planning processes such as power grid expansion. The author[33] proposed stochastic programming for developing a power system network. Moreover, t reliability indices are also considered at the planning stage.

Resilient electrical grid

A resilient grid is a complicated concept with many driving areas such as grid hardening, transient stability, and adequate resources to examine the resilience, like polar vortex[34] and generator governor. The assessment of vulnerability has a goal of locating weak nodes for the improvement of security and resiliency.

The term resilience has various definitions provided by multiple organizations and researchers. According to a UK organization, reliability, resistivity, redundancy, retort, and recovery define a power network's resilience[34]. CENTRE (National Centre for Earthquake Engineering Research) provides the terms "redundancy, resourcefulness, and rapidity consist of the framework of word resilience"[34]. Whereas the MCEER (Multidisciplinary Centre for Earthquake Engineering Research) defined the term as the "ability of social units to mitigate hazards that contain the effects of disasters when they occur and carry out recovery activities in ways that minimize social disruption and mitigate the effects of future disaster"[35]. In 2013, the White House stated the term resiliency as "the ability to prepare for and adapt to changing conditions and withstand and recover rapidly from disruptions"[36]. "The ability to withstand and reduce the magnitude and/or duration of disruptive events, which includes the capability to anticipate, absorb, adapt to and/or rapidly recover from such an event" is the power system resiliency definition stated by IEEE[37]. It is concluded from the literature that the term resiliency defined in the literature varies by two factors, namely, adaptation and recovery. Although the terms resiliency and reliability seem the same. However, the resiliency of a system is the property of the object to return to equilibrium after major environmental disturbances such as natural and intentional disasters.

In comparison, the system's reliability is its ability to supply power to the loads continuously without disruption. The basic difference in resiliency and reliability is given in Table 2[38]. The resilience enhancement work is based on the ability to adapt and ability to recover during the disruption.

Impact modelling of EV load on distribution grid

The penetration of E-mobility is inevitable on distribution grid due to global concern of rising CO_2 emission. Therefore, demand of EV is imperative to map on distribution grid to analyze the weak feeders and adverse impacts. However, the exact load modelling of EV in distribution grid requires the historical behavior of charging/discharging pattern, which eventually does not exist due to its gestation period. Therefore, it is being modelled as probability distribution function (PDF) of random variable derived on traffic pattern and geographical nature in literature[39]. The framework is presented in Fig. 5.

This section shows the impact of EV loading on IEEE-33 bus system. Therefore, to identify the charging/discharging time a PDF function has been formulated based on the collected data on arrival and departure of current vehicle in urban city of India (Dehradun). The PDF(s) to identify the charging time and its loading characteristic, the following assumptions are made as stated below:

- Li-ion battery has been considered as per the current market status of EVs.
- No commercial charging infrastructure has been considered; therefore, it is assumed that charging happens at individual's premises (non-commercial).
- In Indian context TATA EVs have been studied and two models, TATA Tigor and TATA Nexon considered to model the EV load profile.

S. no	Resiliency	Reliability
1	This term is dedicated to the low probability high impact events such as earthquakes, landslides and many more	This term dedicated to the high probability low impact events such as system fault, component failure etc
2	Resilience has various characteristics – adaptive and recovery modes	It is fixed in nature mainly
3	It deals with consumer power interruptions and natural and man-made disasters	It deals with consumer power interruptions
4	Evaluated for specific threats	Evaluated for all the threats
5	Measures the pre, during, and post-disaster effects	Measures frequency and duration of power failure

Table 2. Difference in resiliency and reliability.

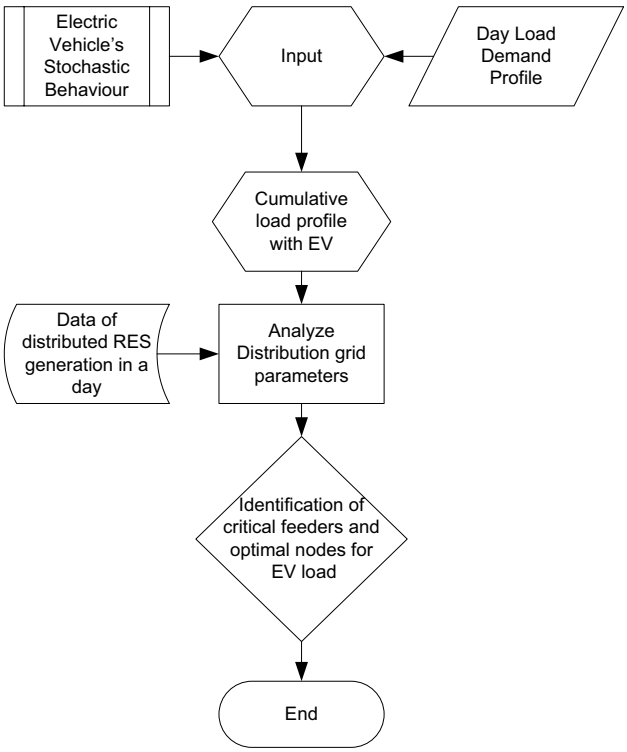

Figure 5. Methodological framework to analyze the EV load impact on distribution grid.

- TATA Tigor has 26 kWh battery capacity and Nexon model comes up with 30.2 kWh and 3.3 kWh home charger unit which takes around 9–12 h for full charge (TATA Tigor) and 12–14 h for Nexon model having conversion efficiency stands approximately at 82%.
- The daily travel distance to model the battery state of charge (SOC) level and required charging energy is derived through running behavior of the present vehicles in urban city of India and a PDF function has obtained.
- The load profile of EVs with respect to charging and SOC's PDF(s) function has been generated using Monte-Carlo simulation.
- The penetration of EVs on IEEE-33 bus system is assumed in three levels, 10%, 20% and 30% on the buses 6, 18, 24 and 30.

Generation of PDF functions

To develop the EV load profile, a PDF function for arrival/departure of EV on weekdays has been generated. To model the traffic pattern, an urban city of India (Dehradun) as a case has been considered. Equations 4 and 5 present the PDF for arrival and departure of EVs[40], respectively and subsequent plots are shown in Figs. 6 and 7.

$$PDF_{Ar} = \begin{Bmatrix} \frac{1}{\sigma_{Ar}\sqrt{2\pi}} e^{-\frac{(t+24-\mu_{Ar})^2}{2\sigma_{Ar}{}^2}}; 0 < t \leq \mu_{Ar} - 12 \\ else \\ \frac{1}{\sigma_{Ar}\sqrt{2\pi}} e^{-\frac{(t-\mu_{Ar})^2}{2\sigma_{Ar}{}^2}} \end{Bmatrix} \tag{4}$$

$$PDF_{Dr} = \begin{Bmatrix} \frac{1}{\sigma_{Dr}\sqrt{2\pi}} e^{\frac{(t-\mu_{Dr})^2}{2\sigma_{Dr}{}^2}}; 0 < t \leq \mu_{Dr} + 12 \\ else \\ \frac{1}{\sigma_{Dr}\sqrt{2\pi}} e^{\frac{(t-24-\mu_{Dr})^2}{2\sigma_{Dr}{}^2}} \end{Bmatrix} \tag{5}$$

Furthermore, the PDF function for distance travel in a day has been created using logarithmic distribution as presented in Eq. (6) and plotted in Fig. 8. Thenceforth, the probability distribution of State of Charge (SoC) of the battery has been obtained from Eqs. (7) & (8). Consequently, the charging profile of EV load for a day has been created from Eq. (9).

$$PDF_{Dis} = \frac{1}{d\sigma\sqrt{2\pi}} e^{-\frac{(\ln d-\mu)^2}{2\sigma^2}}; d = distance\ travel\ in\ km, \tag{6}$$

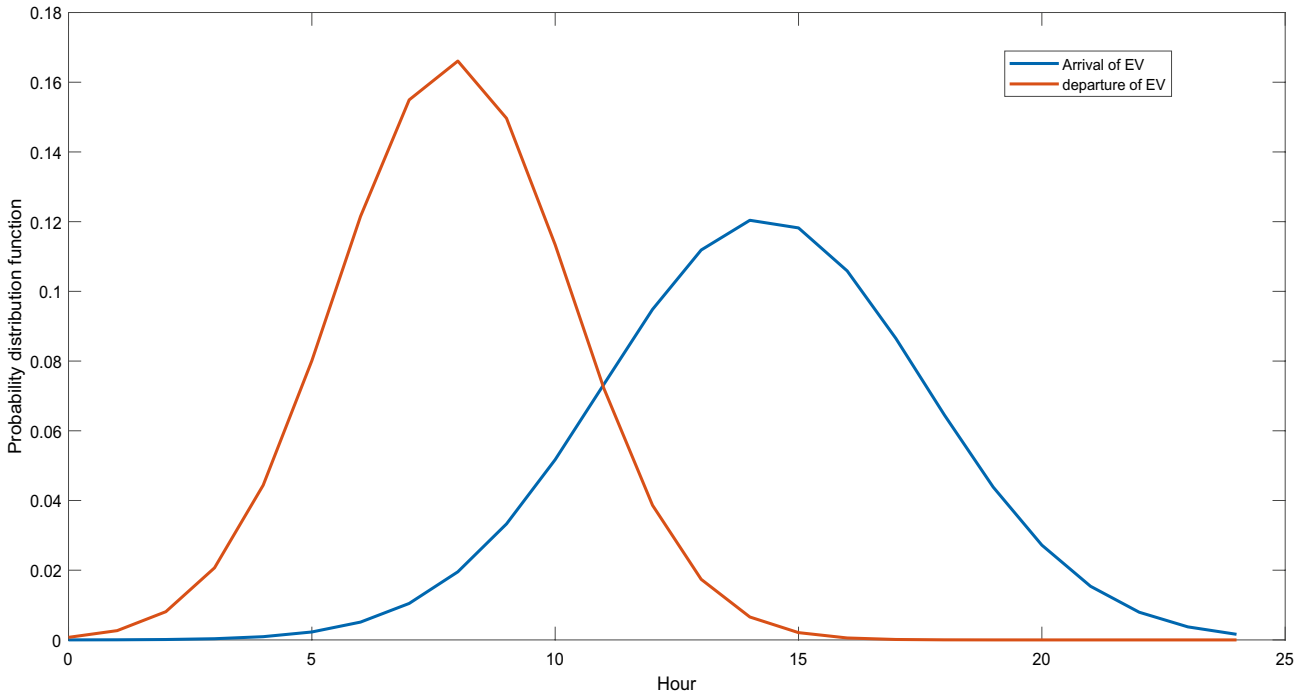

Figure 6. PDF of arrival and departure of EV on weekdays.

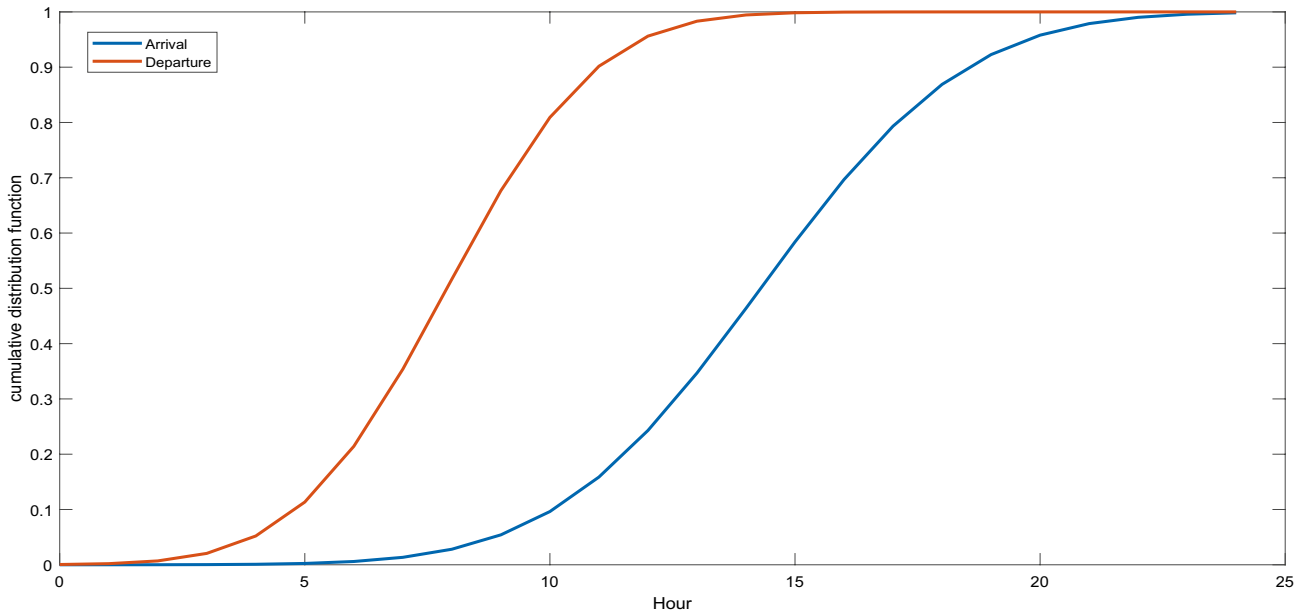

Figure 7. CDF of arrival and departure of EV on weekdays.

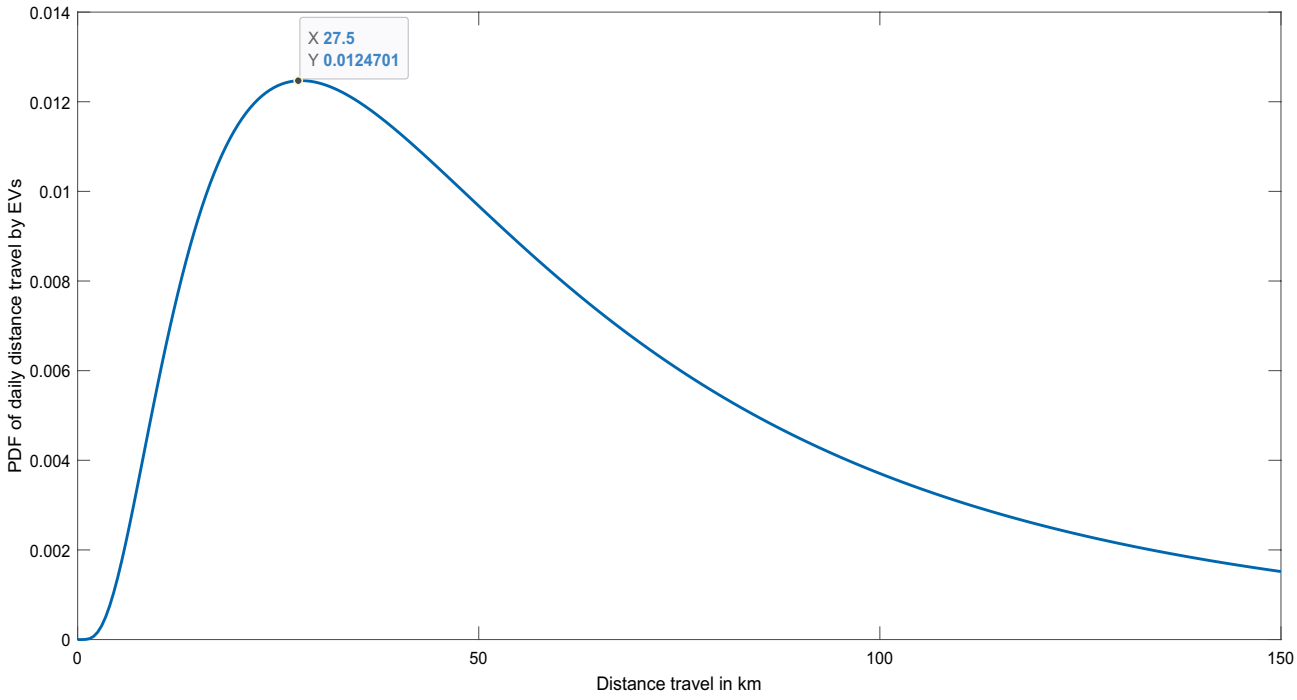

Figure 8. PDF of daily travel distance.

$$SoC = 1 - \frac{d}{R}; R = Range\ of\ EV\ on\ full\ charge, \tag{7}$$

$$PDF_{SoC} = \frac{1}{R(1 - SoC)\sigma\sqrt{2\pi}} e^{-\frac{(\ln(R(1-SoC))-\mu)^2}{2\sigma^2}}, \tag{8}$$

$$T_{charing} = kWh_{battery}(1 - SoC)/(0.82 \times P_{charger}). \tag{9}$$

Load flow profile with EV loading

As stated above, three levels of penetration have been considered viz. 10%, 20% and 30% distributed on four buses. The charging profiles for EVs have been generated through PDF functions and Monte-Carlo simulation. Hence, Fig. 9a–d shows the IEEE-33 bus absolute voltage profile with 10% EV penetration, 24—hour voltage profile, EV bus profile and PV bus profile respectively.

Similarly, Figs. 10a,b and Fig. 11a,b present the voltage profile with 20% and 30% EV penetration respectively for EV and PV bus for visual comparison.

The above voltage profiles shown for different scenarios, evident that EV loading has an adverse impact on the overall system. Moreover, it is imperative to consider the EV load profile during the planning phase for optimal allocation of distributed generation.

Problem formulation for sizing and siting DGs

Objective function

To obtain the optimal DGs sizing and siting, a binary PSO optimization technique[41,42] is used in which a binary variable is taken i.e., 0 or 1 for optimal siting and PSO for sizing. The objective functions (F) are: (i) To minimize the active power loss (ii) Boost the voltage profile.

$$F = f_1 + f_2, \tag{10}$$

$$whereas, min.(f_1) = \sum_{i=1}^{nbr} I_i^2, \tag{11}$$

$$max.(f_2) = \sum_{i=1}^{N} V_i(t) - V_{rated}(t). \tag{12}$$

The Eq. (10) is the combined objective function[43] and the constraints are given in Eq. (13)–(16)[44].

Constraints:

(a) Power flow equations:

$$P_i(t) = V_i(t) \times \sum_{i,j \epsilon N_b} V_j(t)\left(G_{ij} cos\theta_{ij}(t) + B_{ij} sin\theta_{ij}(t)\right), \tag{13}$$

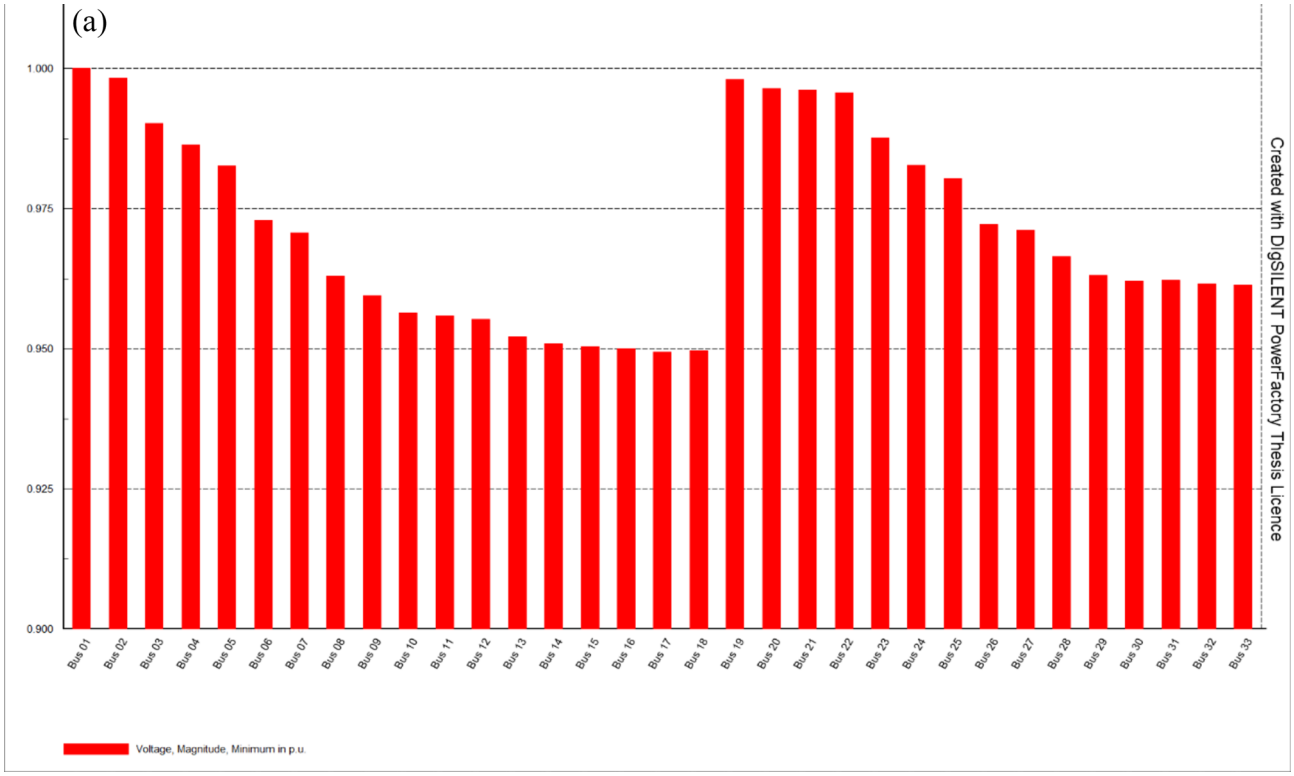

Figure 9. (**a**) Absolute voltage profile with 10% EV penetration. (**b**) 24-h voltage profile of all buses with 10% EV penetration. (**c**) 24-h voltage profile of EV buses with 10% penetration. (**d**) 24-h voltage profile of PV buses with 10% EV penetration.

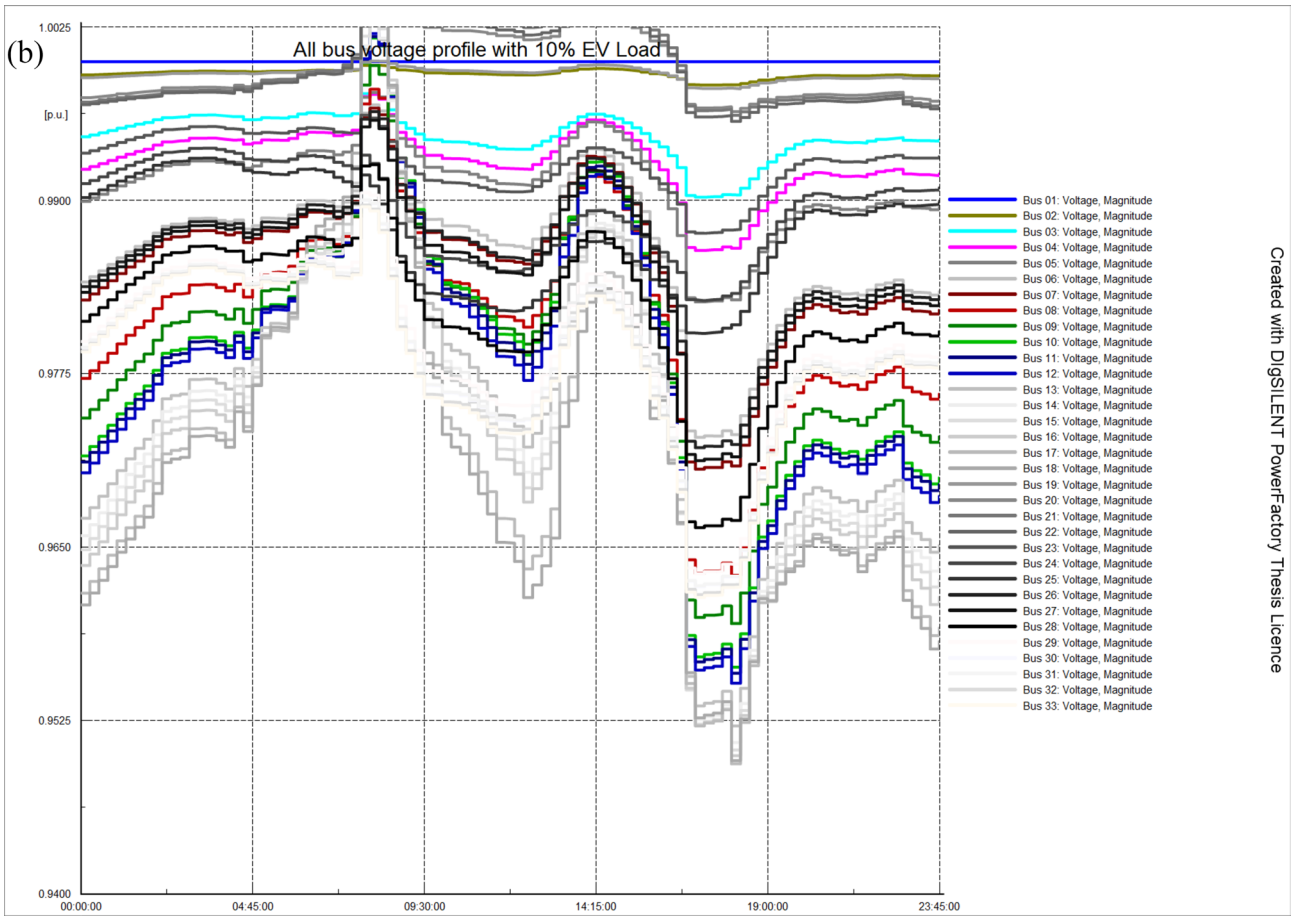

Figure 9. (continued)

$$Q_i(t) = V_i(t) \times \sum_{i,j \epsilon N_b} V_j(t)\left(G_{ij} sin\theta_{ij}(t) - B_{ij} cos\theta_{ij}(t)\right), \tag{14}$$

Whereas, $P_i(t)$ = Real power from ith bus at time 't', $Q_i(t)$ = Reactive power from ith bus at time 't', $V_i(t)$ = Voltage at ith bus at time 't', $V_j(t)$ = Voltage at jth bus at time 't', G_{ij}+ B_{ij} = Element of the Admittance matrix, N_b = Set of buses.

(b) Voltage limits:

$$|V_{min}(t)| < |V_b(t)| < |V_{max}(t)|, \tag{15}$$

V_{min} = Minimum voltage at bus. $V_b(t)$ = Bus voltage at time 't'. V_{max} = Maximum voltage at bus.

(c) Line Loading stability:

$$LL_l(t) < LL_{l,max}(t) \tag{16}$$

$LL_l(t)$ = Line loading of "l" line. $LL_{l,max}(t)$ = Maximum permissible loading of "l" line.

Sizing siting for IEEE-33 bus system

To validate the proposed optimization algorithm, the IEEE-33 bus system having 12.66 kV radial distribution system is taken as a reference. The heatmap of IEEE 33 bus with optimally placed DGs (PV) is shown in Fig. 12.

A combination of binary PSO (for siting) and PSO (sizing) has been applied to find the optimal allocation of DGs for IEEE-33 bus system. Table 3 presents the optimal sizing and siting of DGs for IEEE-33 bus system. Figure 13 shows that the voltage profile has been improved with the optimal PV placement. It is concluded that the generation from PV will suppress the stress on the grid and hence improve the voltage profile.

DG allocation with Quasi dynamic simulation

Quasi dynamic simulation is used to perform multiple load-flow calculations with time-step sizes defined by the user. In the presented work a time step size of 15 min is taken. Moreover, 15 min step size is also being used to match the generation and demand by state load dispatch center (SLDC), India. To replicate the practical scenario, load profile of urban city of India (Dehradun) has been considered for summer season as depicted in Fig. 14.

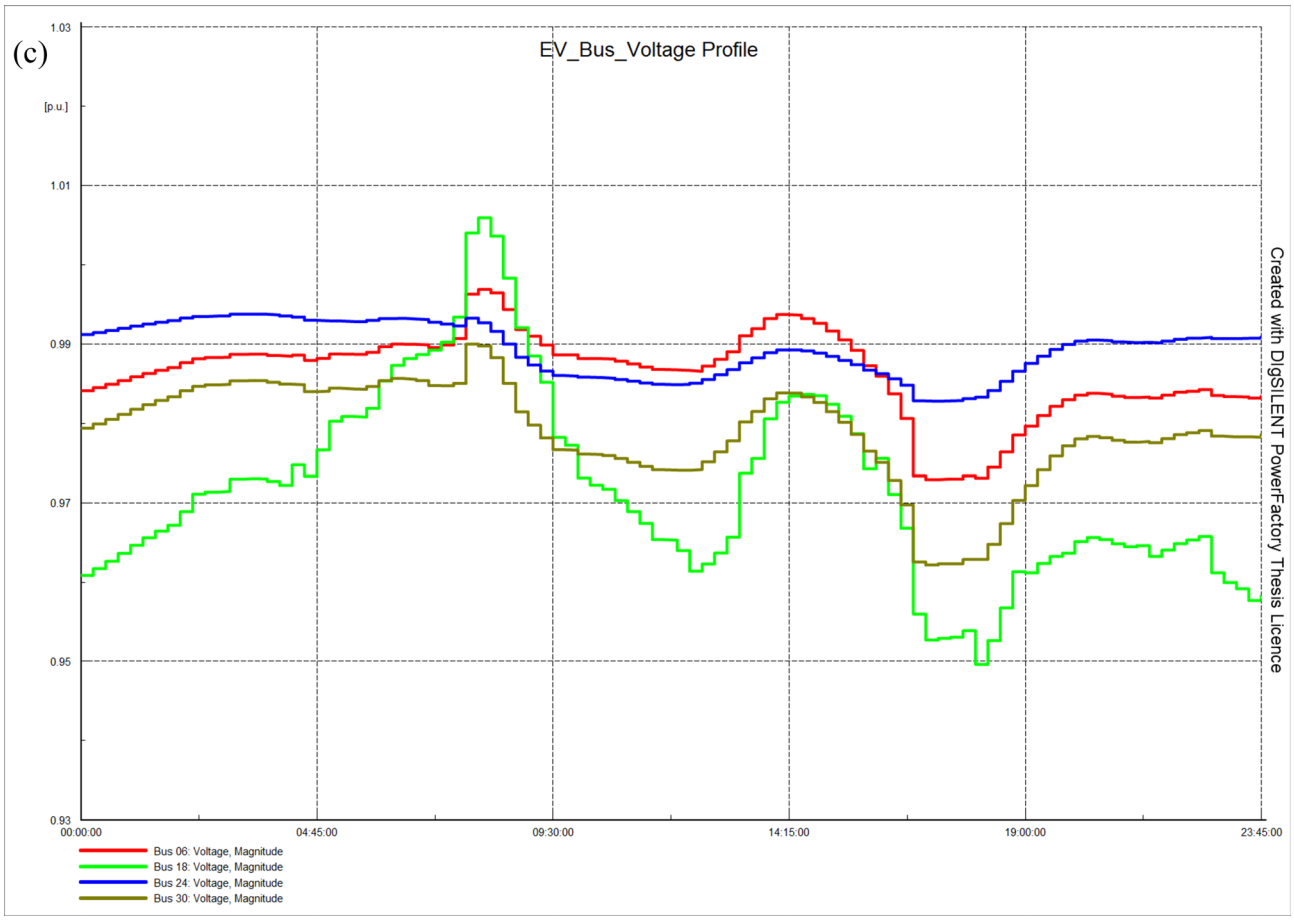

Figure 9. (continued)

Moreover, the solar PV per unit output on a sunny day for the said region (Dehradun, 30.3165° N, 78.0322° E) is considered for quasi-dynamic simulation and shown in Fig. 15.

Comparing Figs. 13 and 16, it is taken out that one day profile shows very less improvement in voltage profile with PV as load demand stays at its peak even after irradiance goes down. Therefore, it is recommended to integrate DGs (solar PV, wind etc.) with battery storage system to curtail the intermittency of solar PV generation during daytime and hence improving the voltage profile throughout the day.

However, to boost the voltage profile and to cater the PV intermittency; DG with battery storage placement is recommended. Thenceforth, the optimization algorithm has been run on optimally integrated PV IEEE-33 bus system for sizing and siting of battery storage. After 10 iterations, two locations for battery storage have been identified on Bus-21 = 248 kW and Bus-18 = 472 kW. Furthermore, per-unit optimal charging/discharging profile (24 h) of the battery is shown in Fig. 17.

Also, the voltage profile of the one-day of IEEE-33 system for PV integrated bus is shown in Fig. 18. In comparison, one day voltage profile of IEEE-33 system for PV integrated bus with optimal charging/discharging of storage (24 h) is shown in Fig. 19. Hence, the overall improved voltage bus profile with PV and storage is shown in Fig. 20.

Impact of extreme event on an urban Indian electric grid

The objective of this section is to demonstrate the effectiveness of machine learning techniques to model the impact of a natural disruption (earthquake) on electrical infrastructure. Therefore, an urban Indian electric distribution grid of Dehradun city (high seismic zone) with critical loads is considered and simulated on power factory software, as shown in Fig. 22. The data for distribution grid modelling has been presented in Annexure 1[12]. Therein, for the impact on grid, earthquake natural disasters are considered as an extreme event in the paper. Five-year data is collected from the years 2017 to 2021 to generate the earthquake profile. The collective data set is provided in Annexure 2, which shows the magnitude and the event depth (in km). The adopted methodology to map the earthquake profile and subsequently generating the damage state of taken case study has been presented in Fig. 21. A complete grid has been simulated on PowerFactory[45] as per Annexure 1, single line diagram (SLD) and voltage profile without damage for 24 h is shown in Figs. 22 and 23, respectively.

Figure 23 shows the 156-bus voltage profile with load scalability and solar PV variation in normal conditions. It is evident that the lowest voltage goes up to 0.9310 p.u. during late morning to afternoon.

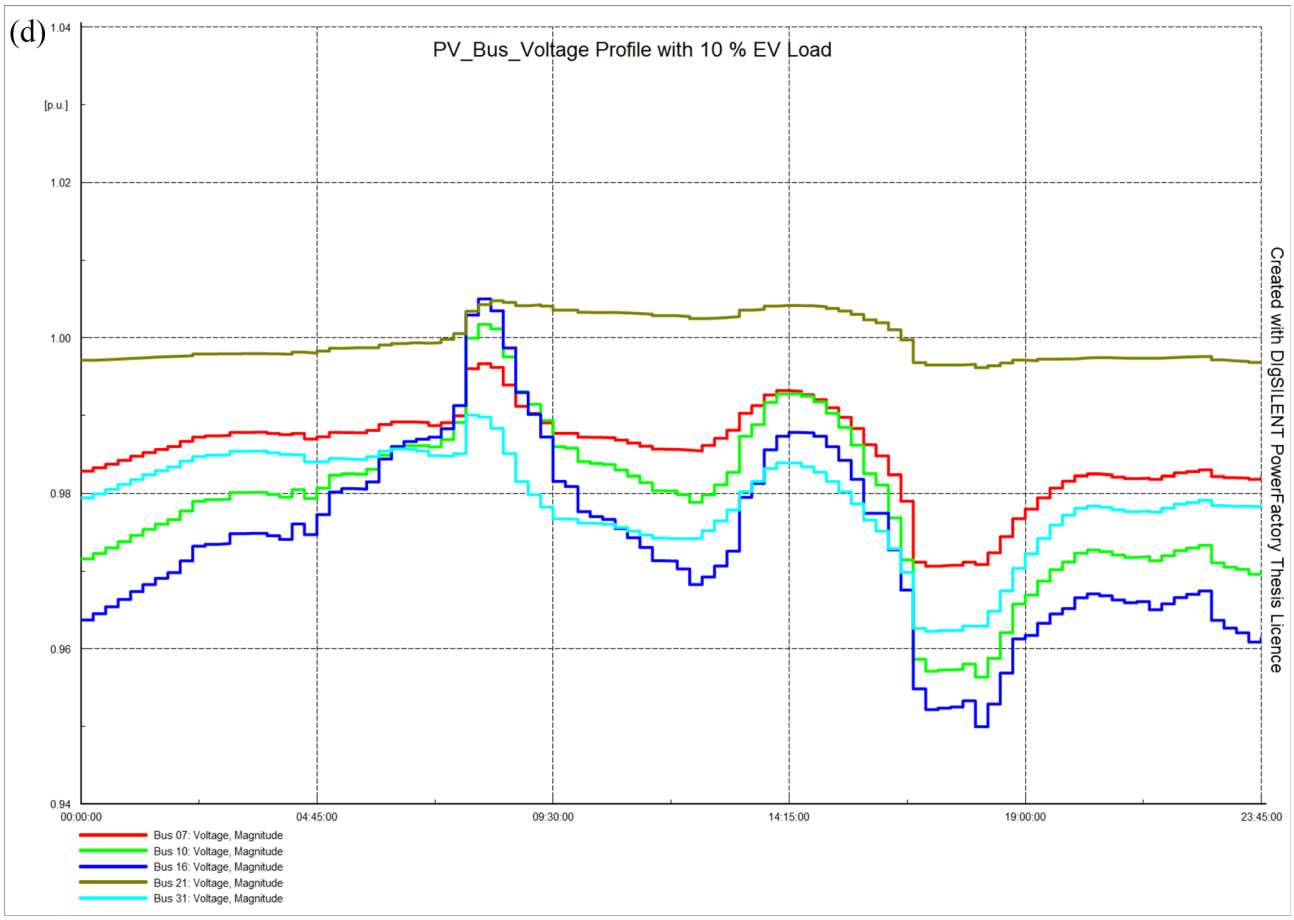

Figure 9. (continued)

Clustering of network

The clustering of the entire distribution grid has been done on population density, tourism aspect and connected load density. The datasheet is provided in Annexure 3. Several papers in the literature show the optimization process duly accounting clustering like in Ref.[46], authors have presented EGC-CMOPSO optimization methodology based on clustering. However, in the presented manuscript, the clustering has been performed by using supervised k-means algorithm and the platform used for visualizing geospatial data is the python library- folium[47]. The total number of clusters required is given as an input to k-means algorithms. This optimal number of clusters was obtained from elbow curve during the grid transition, as shown in Fig. 24. The obtained optimal number is 8 (Fig. 24a); therefore, the optimal clustered zones within the Dehradun distribution grid are eight as shown in Fig. 25. In Fig. 25, the circle denotes the clusters, and the same colour circles represent all belonging to same clusters. Moreover, the distribution lines along with optimal clustered zones are shown in Fig. 26.

Simulation of the proposed methodology on an urban Indian electric grid of Dehradun city

The impact analysis of natural disaster has been performed onthe distribution lines of study region (Dehradun grid) with tectonics plates modelled using Python as shown in Fig. 27. The last five years earthquake locations are show in Fig. 28 (diameter of circles represents the magnitude). Thenceforth, to identify the damageability of the infrastructure (11 & 33 kV feeders), peak ground acceleration (PGA) values are calculated for finding the ground motion.

The values of PGA are calculated by using Eq. (17)[48] and the PGA value distribution curve shown in Fig. 29.

$$PGA = 0.02938.e^{1.19950M}.\left[R + 0.14667.e^{0.69689M}\right]^{-1.73413}, \tag{17}$$

where M is the magnitude of the earthquake. R is the distance between one point in the source of the earthquake.

However, Fig. 29 shows the random distribution of PGAs, so after using A/B probability test function, the distribution of PGA value is obtained as shown in Fig. 30.

Risk value assessment

Risk value denotes the damage state of the substation. Based on the risk value, the damage states are classified into five states: High impact, Moderate Impact, Normal Impact, Low Impact and Very low Impact. The range used

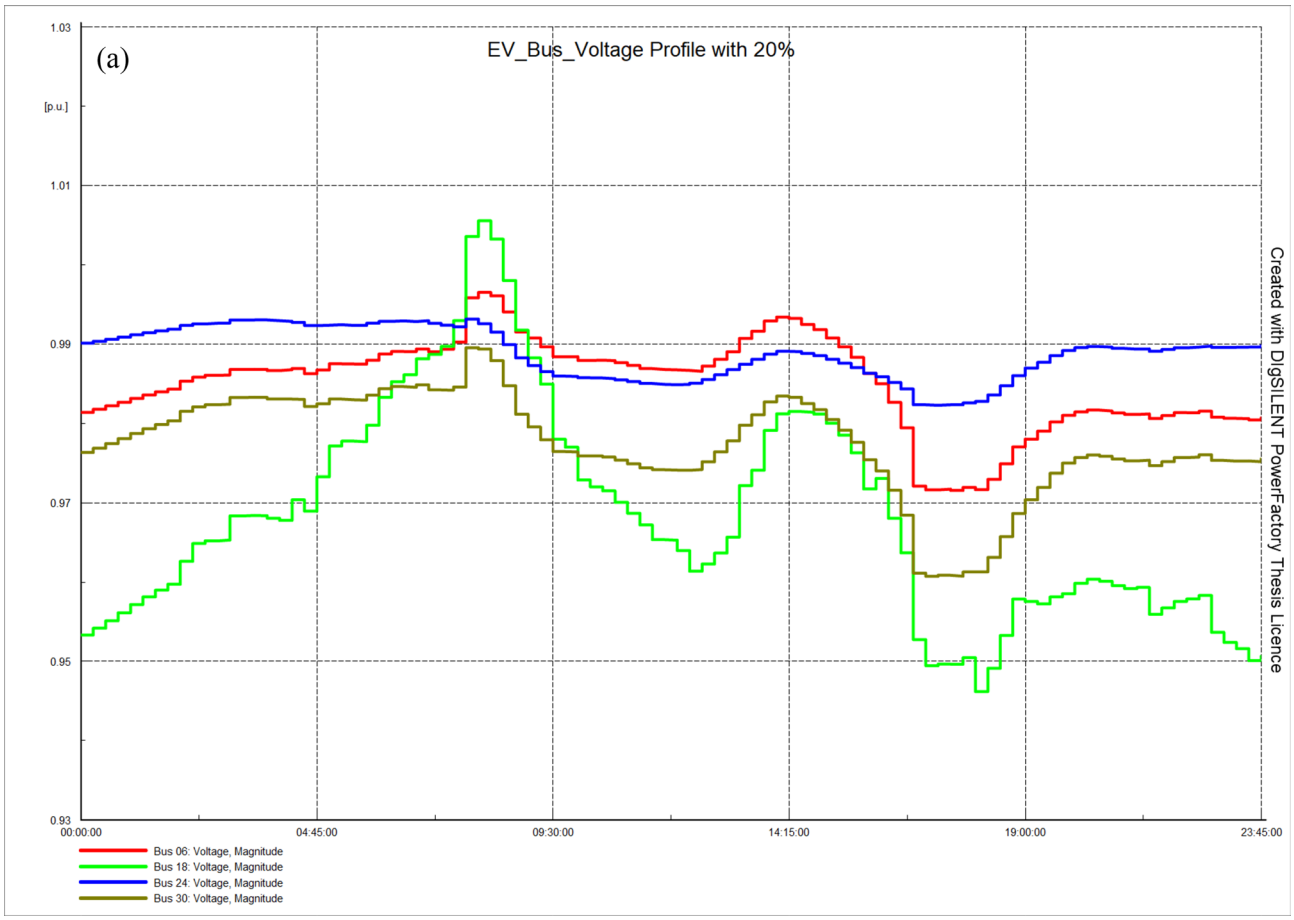

Figure 10. (**a**) 24-h voltage profile of EV buses with 20% penetration. (**b**) 24-h voltage profile of PV buses with 20% EV penetration.

for the classification is shown in Table 4 and the respective curve is shown in Fig. 31. However, it is concluded that if the PGA value is high it results in high station risk value. Therefore, the final practical values obtained in the python platform is the cumulative result of the PGAs of all stations and shown in Fig. 32. In addition, the risk value of the stations with associated cluster is mentioned in Table 5.

Thenceforth, after identifying the damage lines for the taken study grid, a closed loop process within python algorithm and PowerFactory model has been performed as per Fig. 22 to eliminate damage lines from operational state. Consequently, the affected grid after impact analysis and 24-h voltage profile of the grid has been shown in Figs. 33 and 34 respectively. The gray region in Fig. 33 shows the affected lines.

Figure 35 presents the comparative visualization of taken distribution grid state before and after an event. It is evident that a natural disaster can severely affect the vulnerable distribution grid. However, as per present needs, placement of energy storage devices is being implemented in distribution grid to cater the intermittent nature of RES and stochastic loading of EV. Therefore, the presented study substantiates that to build the resilient futuristic grid, RES and storage planning should consider the natural/manmade disruption analysis. The handy machine learning/AI tools are well versed to deliver the results when combined with conventional load flow analysis software tools. Consequently, presented grid case study substantiates that if adverse impact analysis due to any catastrophic event would have been considered in planning phase than engineers can have contingency plan (e.g. parallel critical feeder lines, DGs allocations) to improve the load served after an event which overall improves resiliency.

Conclusion

The presented paper proposed the planning framework for a resilient electric distribution grid. To achieve the stated objectives, firstly, a load flow analysis of IEEE 33 bus system is simulated that shows the voltage profile without any DG placement in the distribution system. Then, using optimization, an optimal allocation of DG in the system shows the improvement of voltage profile. Later, a quasi-dynamic simulation is done to analyze the one-day behavior of PV and load. The quasi-dynamic simulation shows that the voltage profile after integration of DG results in improvement of voltage, however up to an extent. Therefore, it is concluded from comparing the voltage profile of the IEEE 33 bus system with different scenarios for reducing the stress on the grid that the optimal placement of DG with battery storage in distribution system is the best solution.

Moreover, earlier, the reliability of the electrical grid was the foremost key performance index. However, recent developments like RES infusion and EVs adaptability demand a sustainable and stable electrical grid.

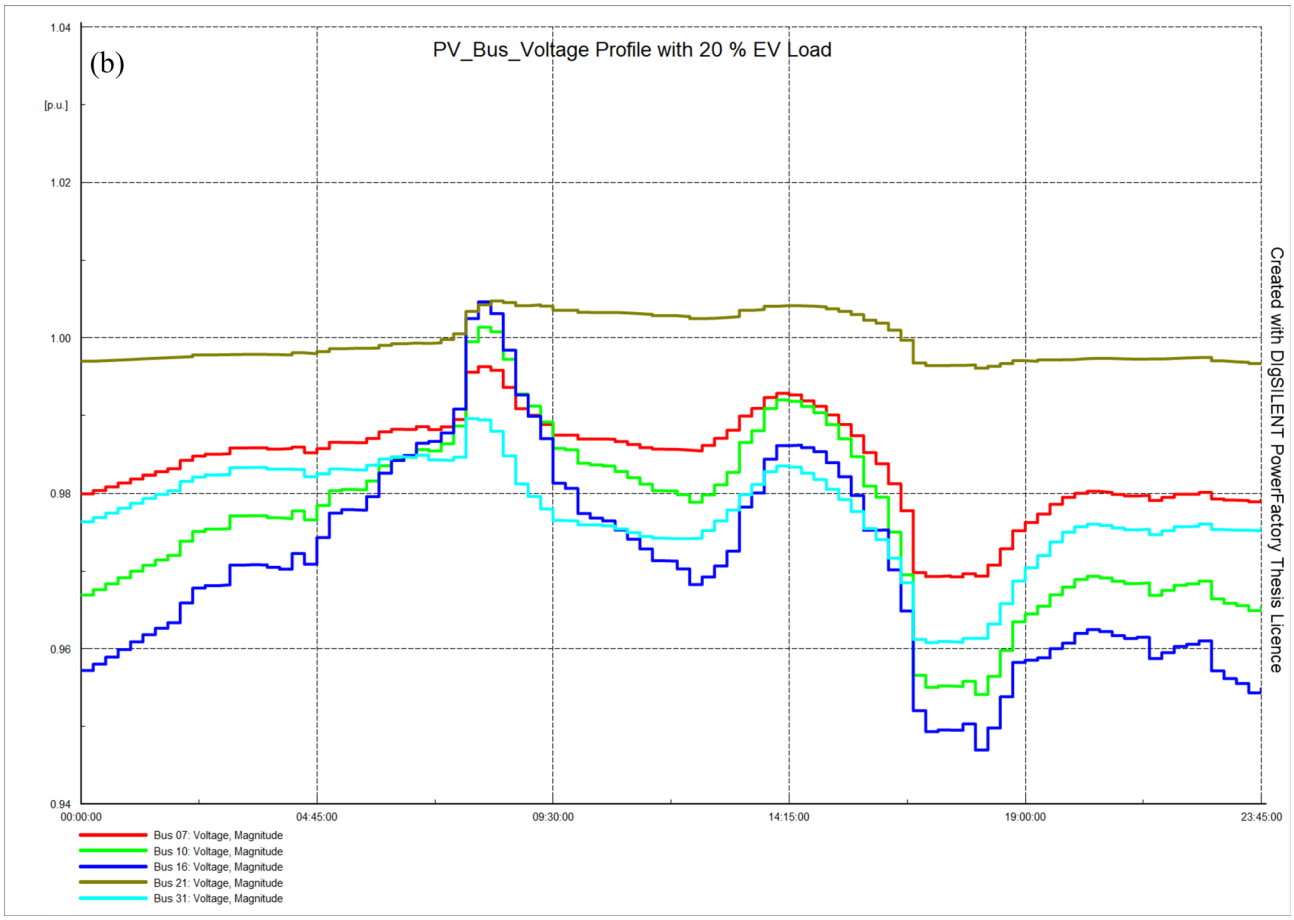

Figure 10. (continued)

Besides, a resilient index has become a key indicator in dealing with catastrophic events' impact on the electrical grid. Therefore, the presented work elaborates on the power system resiliency concept and also differentiates the reliability. Subsequently, it is concluded that EVs load can be mapped on the electrical distribution grid through the probability of random variables. Therefore, the probability density function (PDF) to map EV density has been formed based on growth projection and the socio-economic adaptability of EVs. The impact of the catastrophic event on the distribution grid has also been addressed. However, the work shows an approach to analyze the grid degradation after a catastrophic event for an earthquake-prone, mixed terrain India's urban city electrical distribution grid. The approach considers the optimal clustering of the entire distribution grid based on demand, population, and social index. The smart grid definition is changing every day, and the distribution grid has become the most dynamic part of the smart grid due to inclusion of RES and EV loading. Therefore, it is imperative that planning engineers should consider the natural/manmade disruption analysis for the resilient futuristic grid. The presented paper shows merely an approach which has many limitations like lack of actual data on EV charging pattern, available land mapping with grid, access to charged lines during & after disastrous events, location of underground cables (the impact analysis would have different approach) and the variables list goes on. However, this non-linearity will keep on growing moving forward, therefore, including these dimensions as they appear in future will enhance the degree of resiliency for our electrical infrastructure and grid.

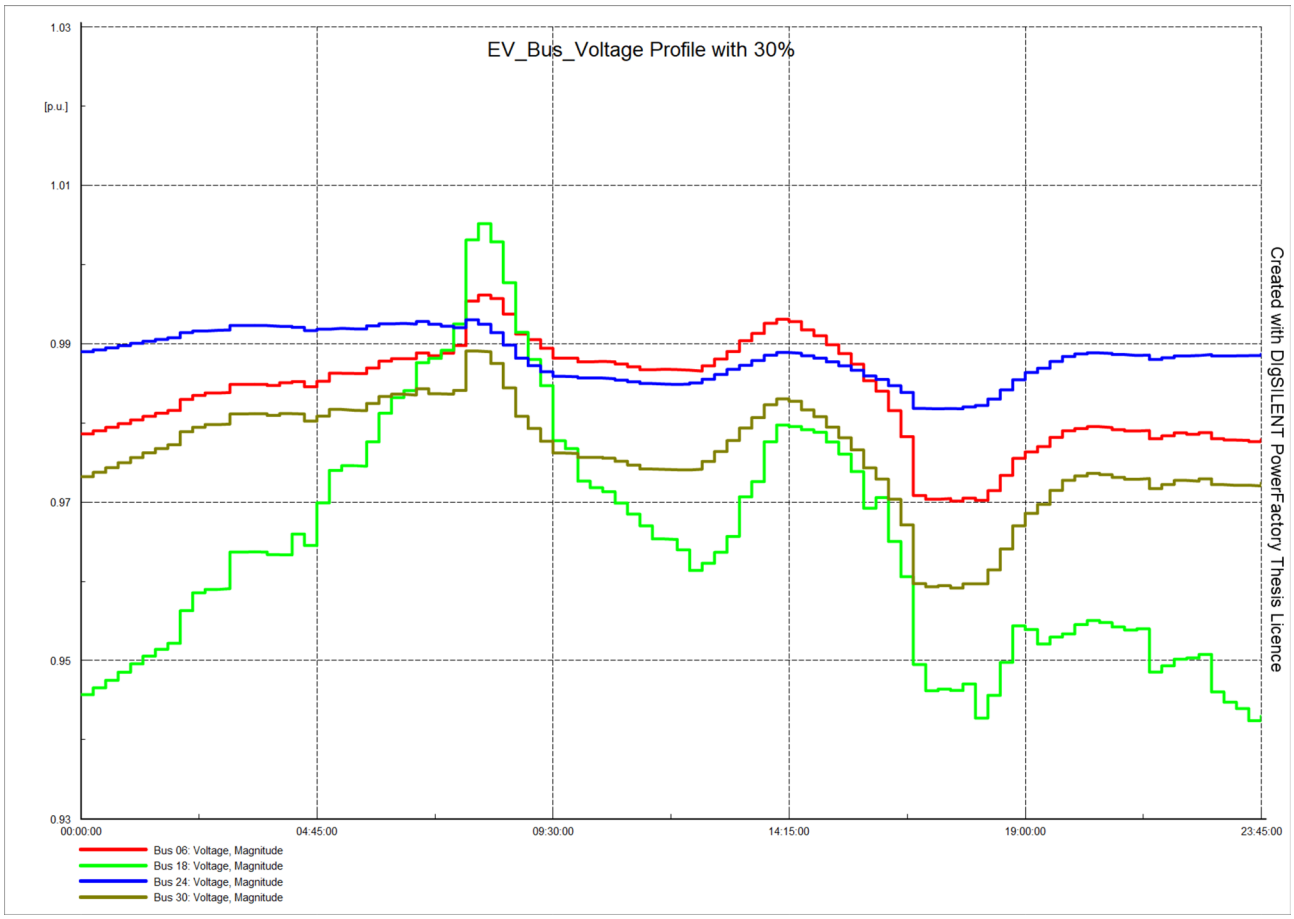

Figure 11. (**a**) 24-h voltage profile of EV buses with 30% penetration. (**b**) 24-h voltage profile of PV buses with 30% EV penetration.

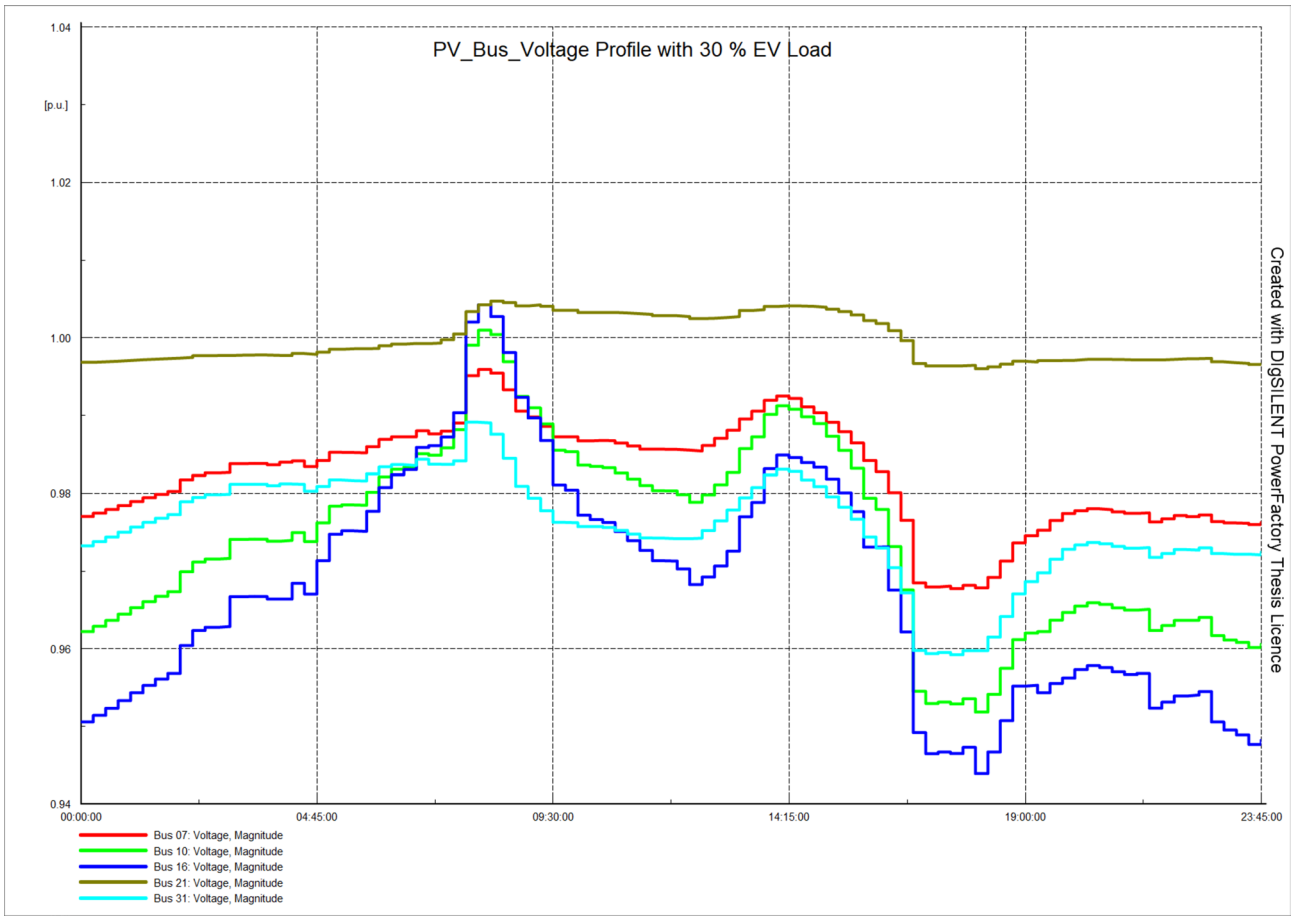

Figure 11. (continued)

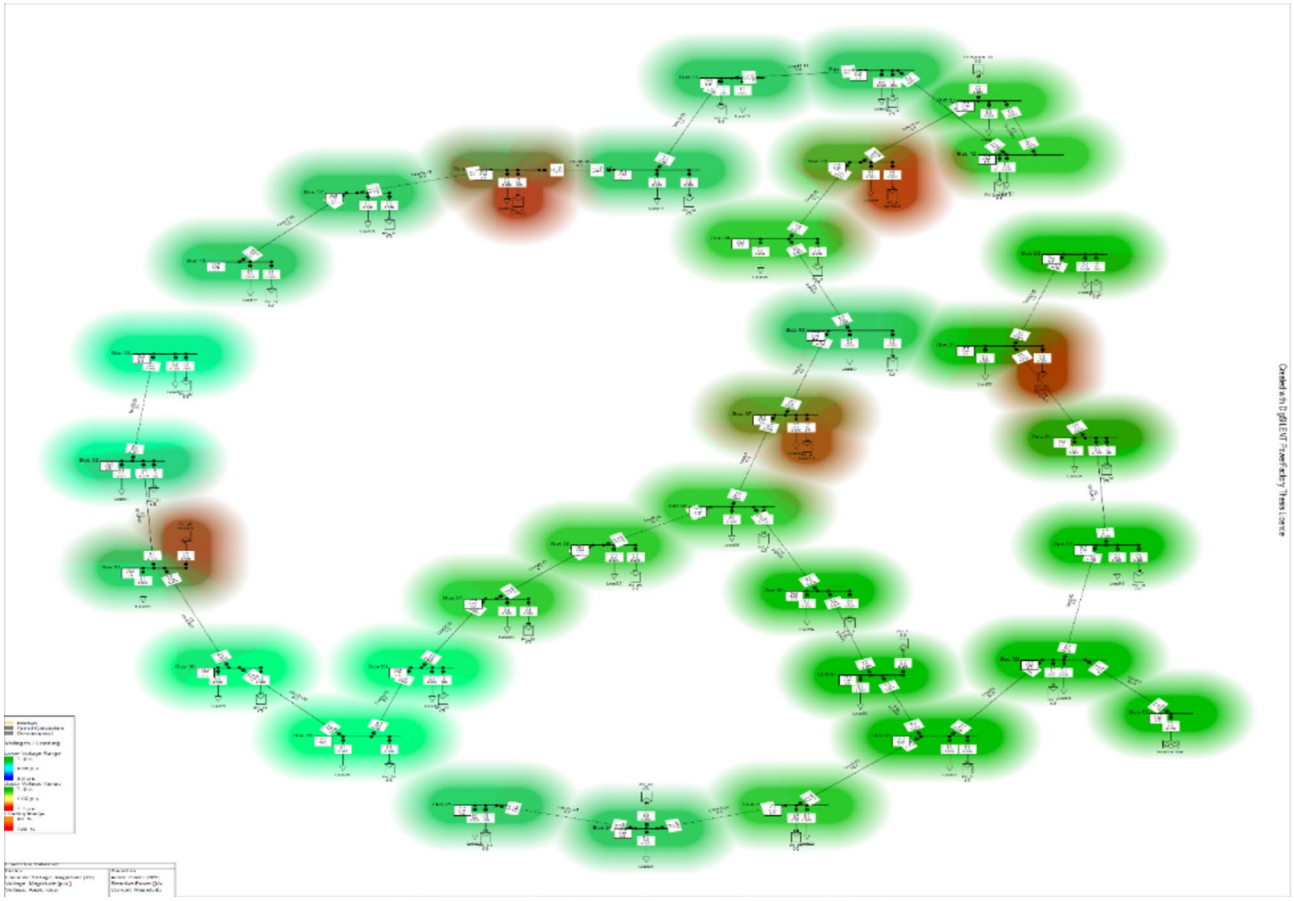

Figure 12. Heat map of IEEE-33 system with PV placement.

Parameters	Outcome
Best cost obtained from PSO	[2766977.945]
Total % real power loss in kW	127.648
Total % reactive power loss in kVAR	90.567
Total % voltage deviation	11.720
Total size of RES to be installed	3.464 MW
Total no of RES	05
Best location obtained from PSO	[7, 10, 16, 21, 31]
Bus 7	0.955 MW
Bus 10	0.642 MW
Bus 16	0.422 MW
Bus 21	0.821 MW
Bus 31	0.624 MW

Table 3. Optimal DGs sizing and siting on IEEE-33 system.

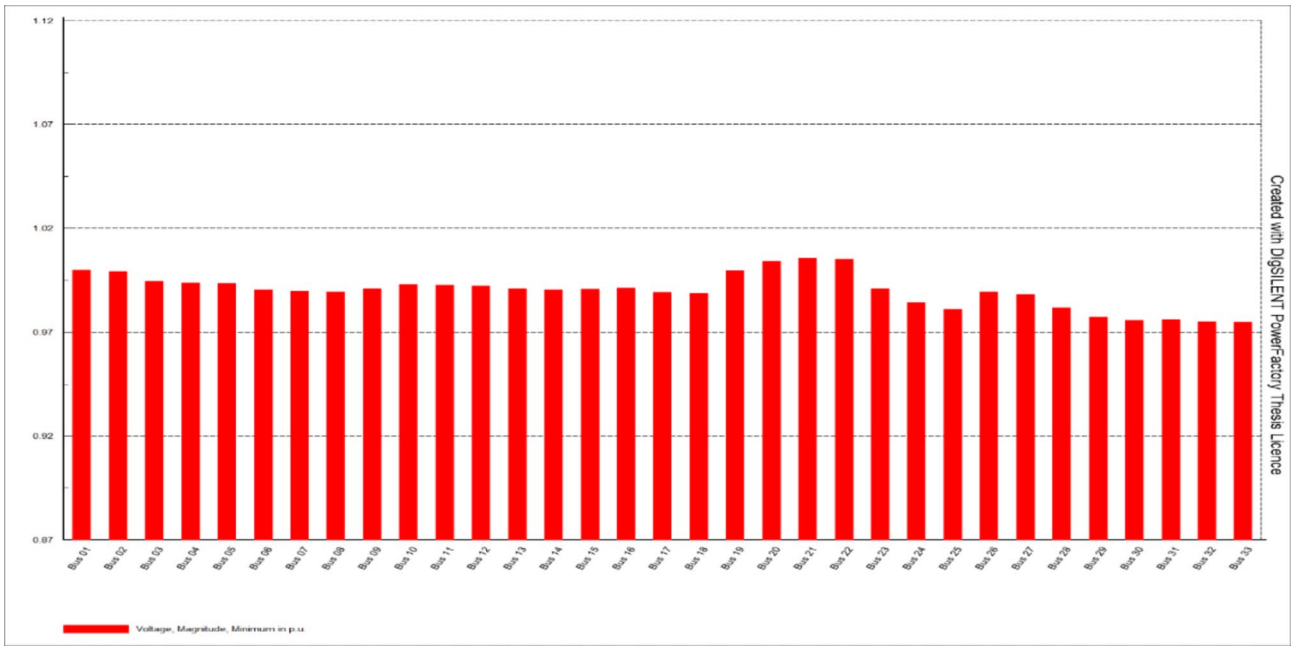

Figure 13. IEEE-33 bus voltage profile with PV placement.

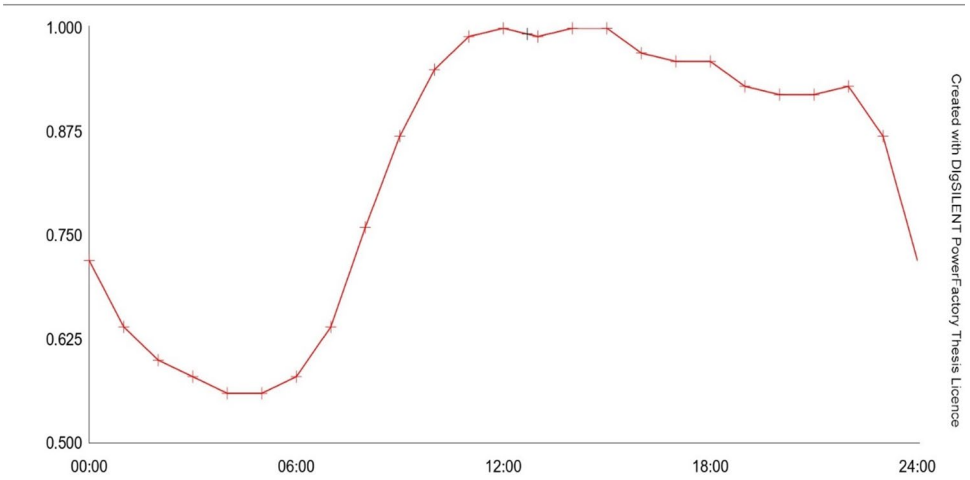

Figure 14. One day per unit load profile.

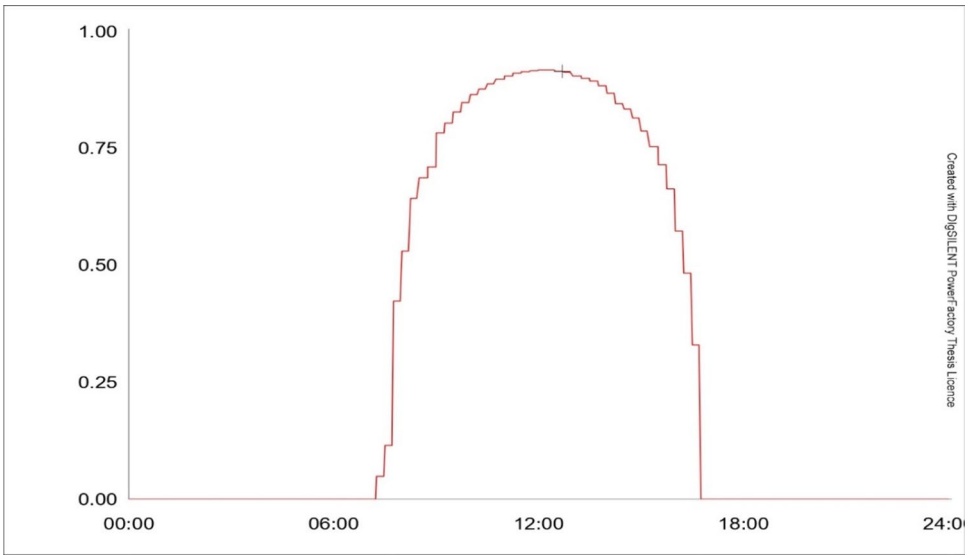

Figure 15. One day per unit PV output profile.

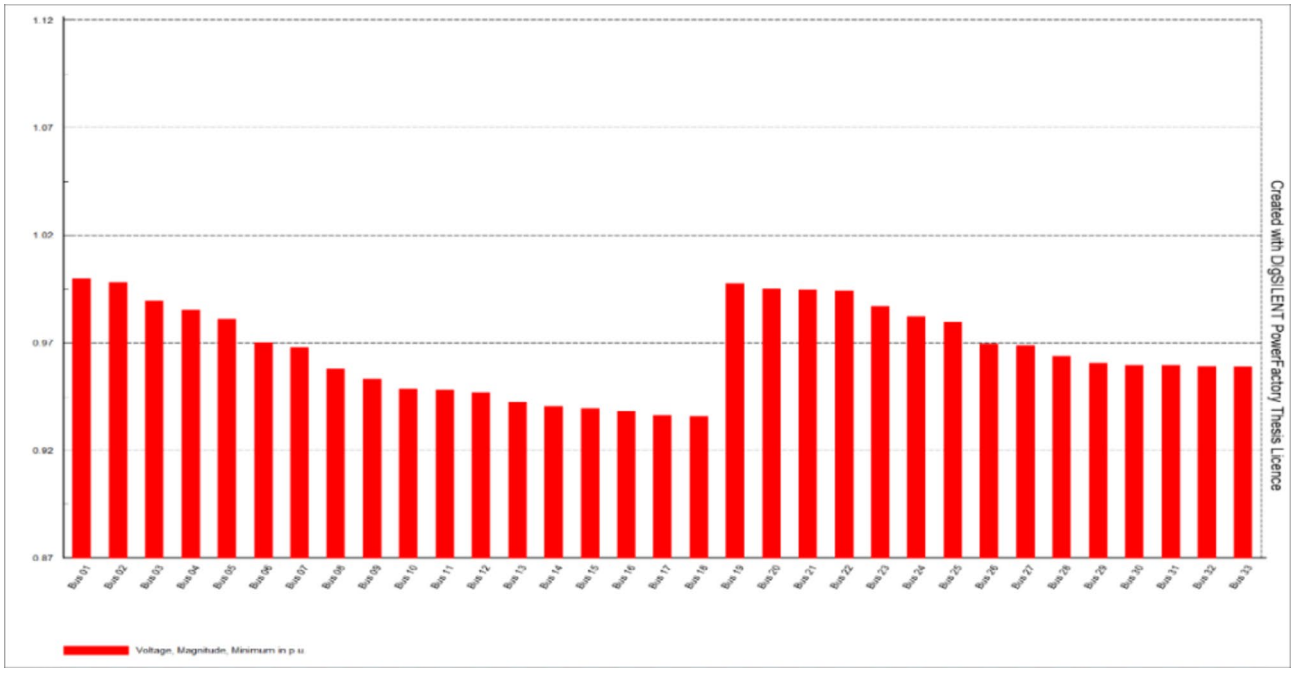

Figure 16. Voltage profile of IEEE 33 Bus with load and PV variability.

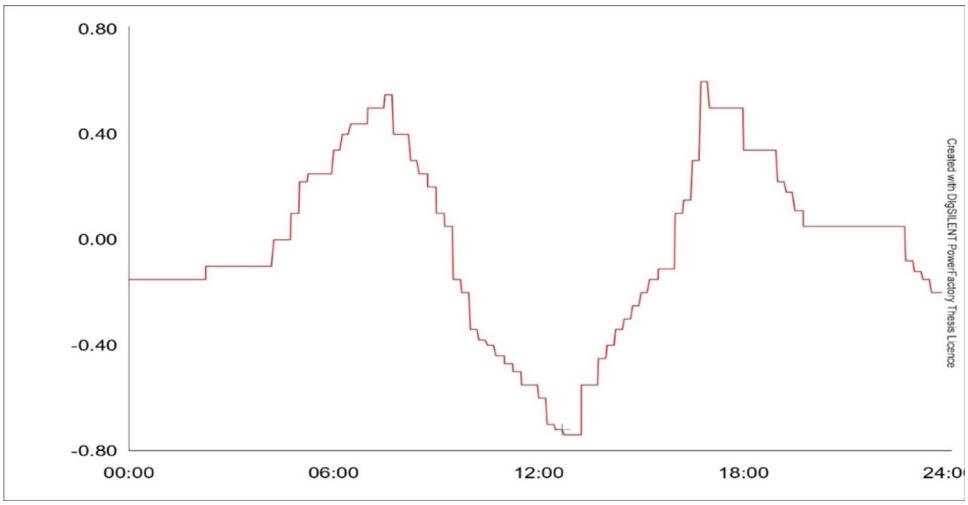

Figure 17. Optimal charging/discharging profile (24 h).

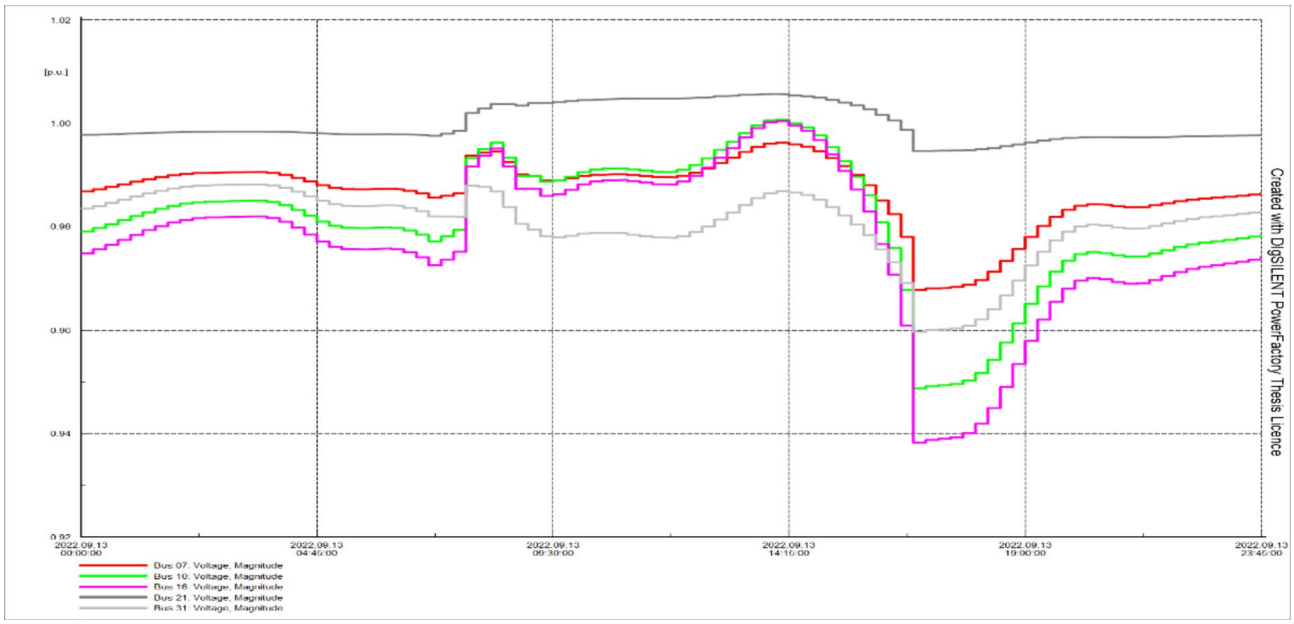

Figure 18. Voltage profile of PV bus (24 h).

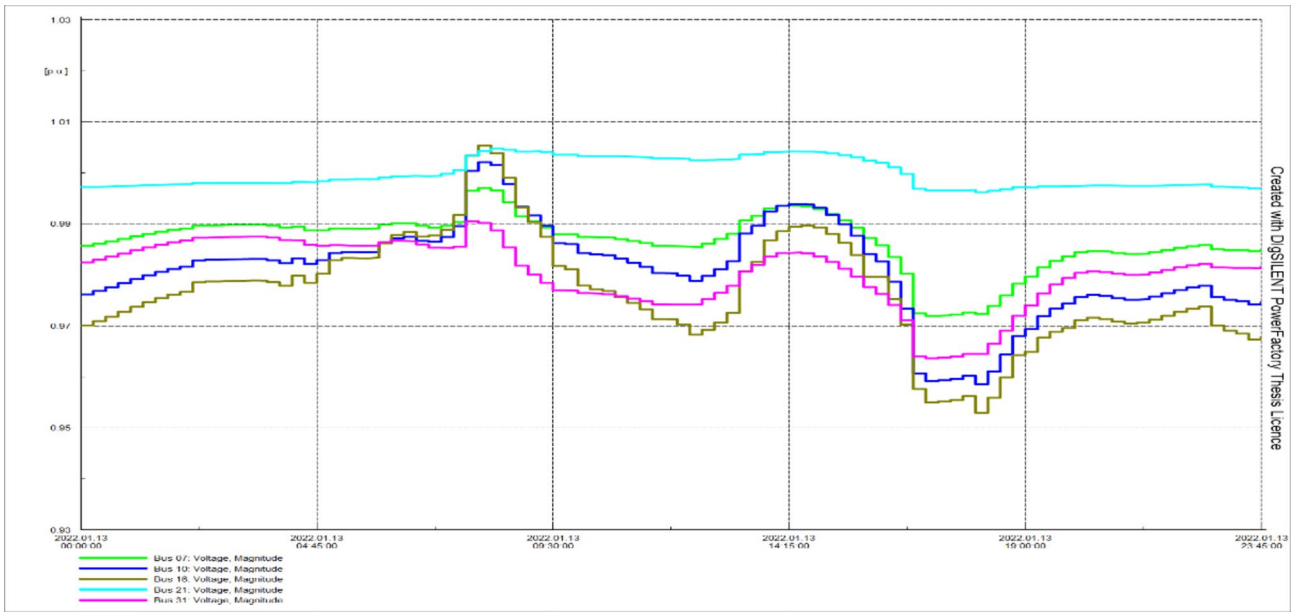

Figure 19. Voltage profile of PV with storage (24 h).

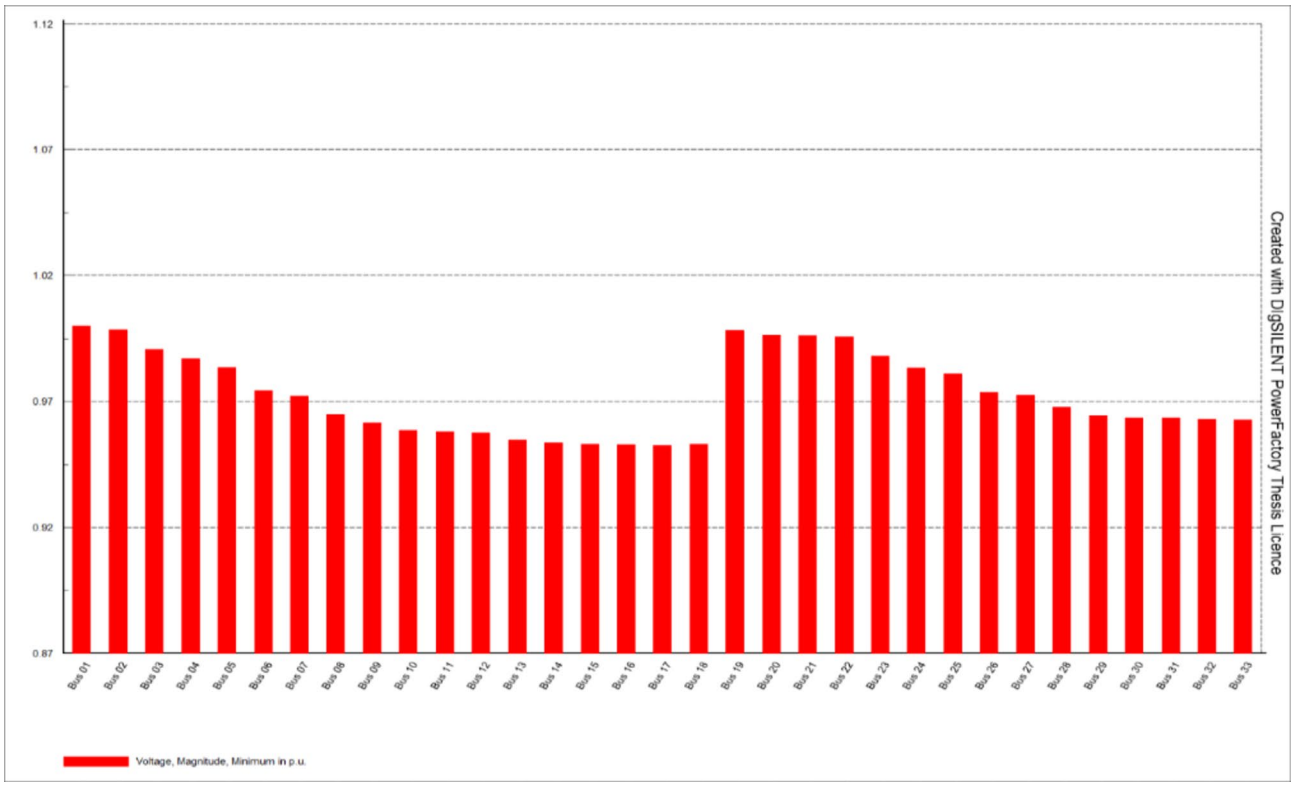

Figure 20. Overall bus profile with PV and Storage (24 h).

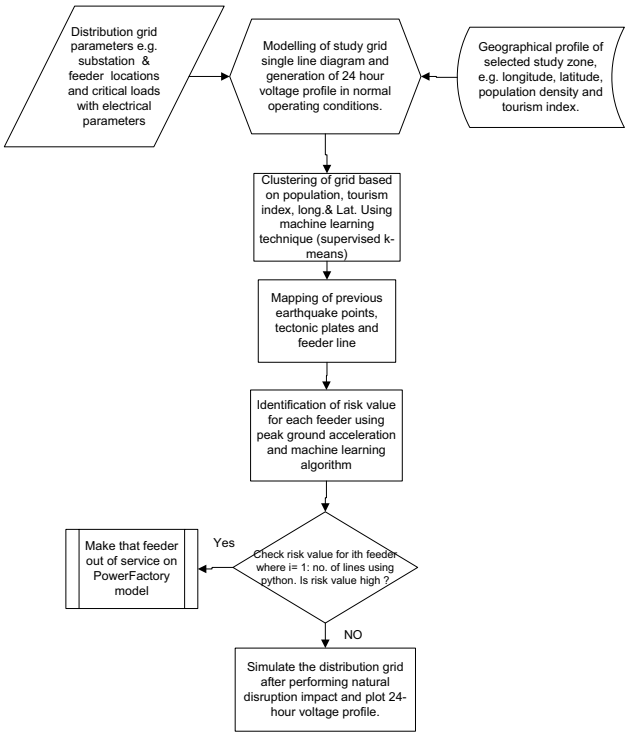

Figure 21. Methodological flowchart to model the grid after impact analysis.

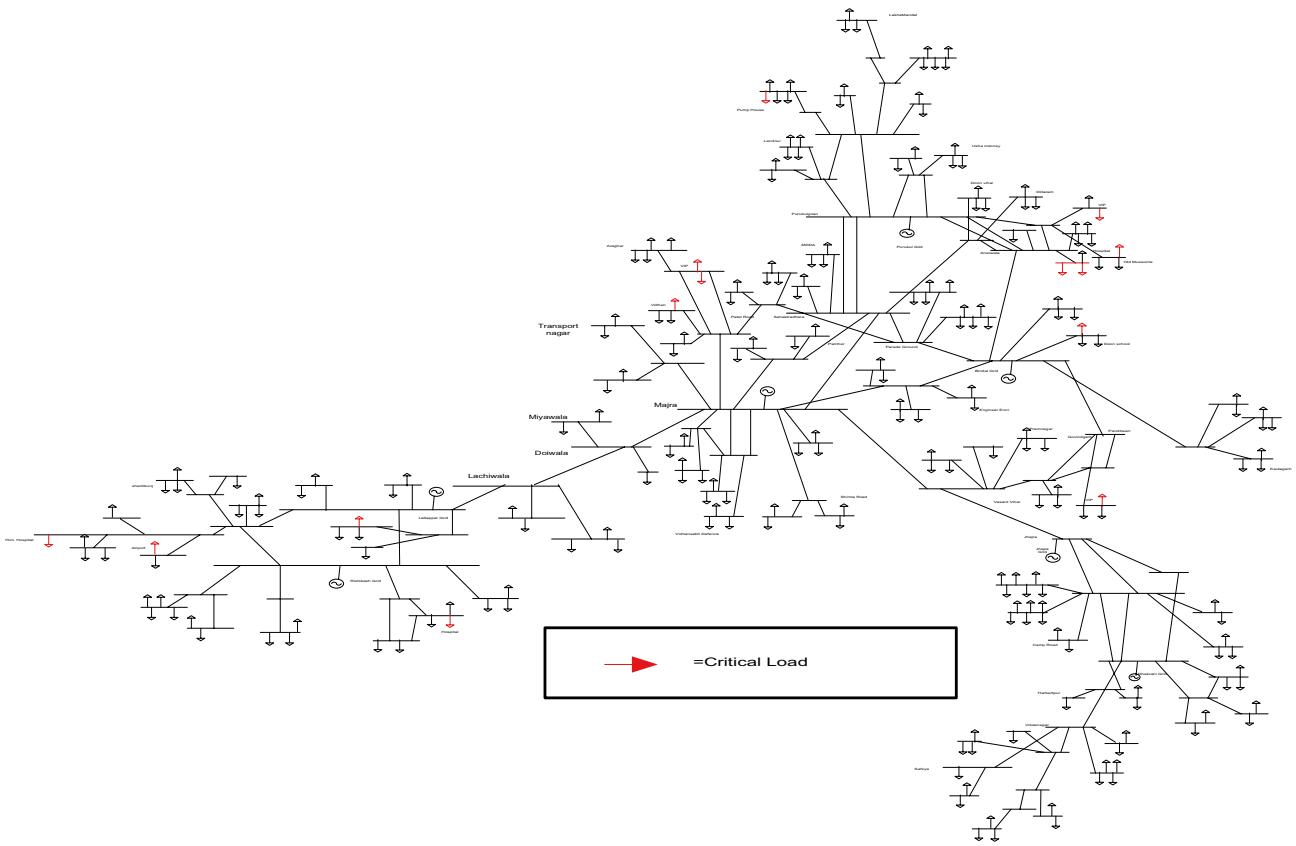

Figure 22. Dehradun city's grid single line diagram with critical loads.

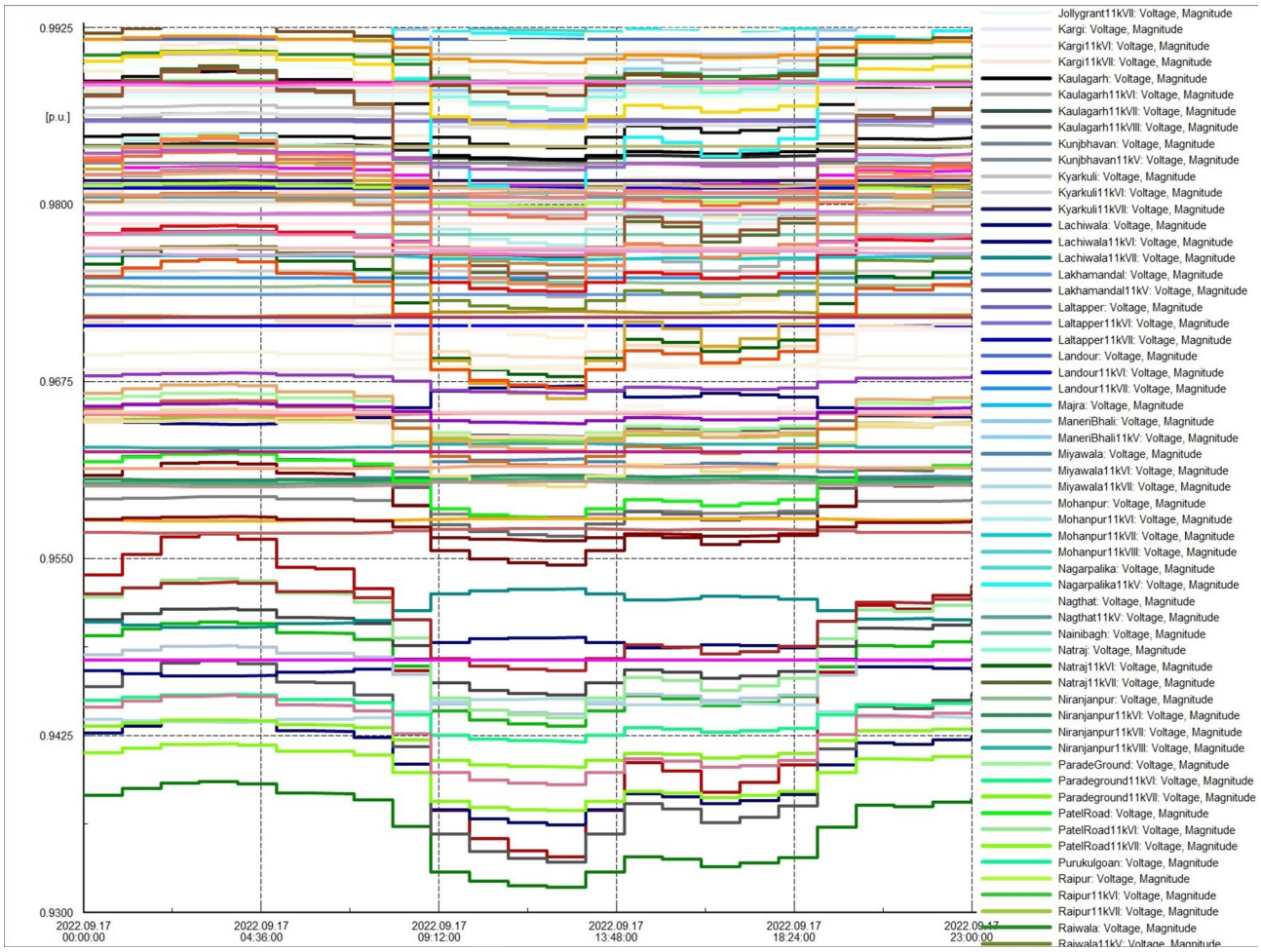

Figure 23. Dehradun Grid profile without natural disruption damage for 24 h.

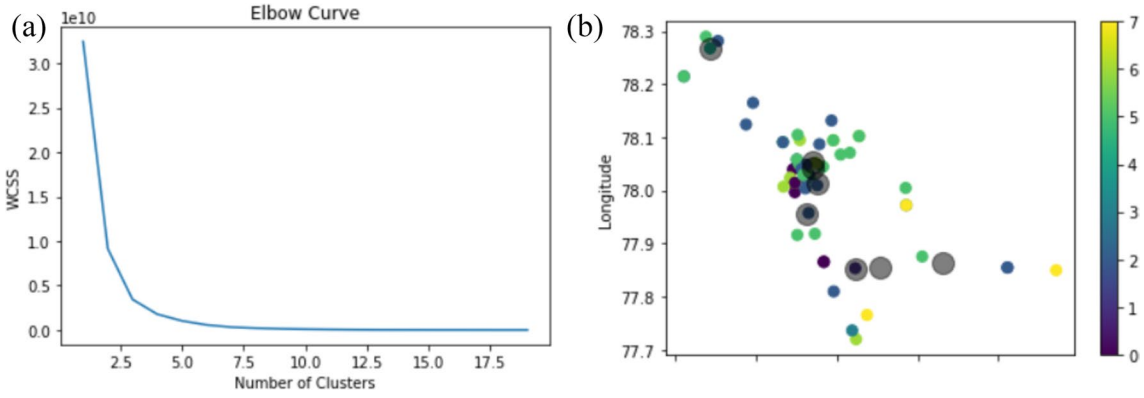

Figure 24. (**a**) Elbow curve to find optimal clusters. (**b**) Clusters based on (latitude, longitude, population, tourism index, critical load).

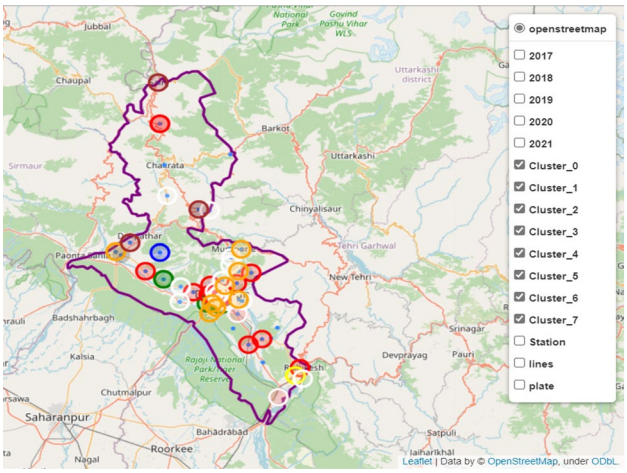

Figure 25. Optimal clustered zones within the Dehradun distribution grid[47], map generated using Leaflet data by openstreetmap wiki.

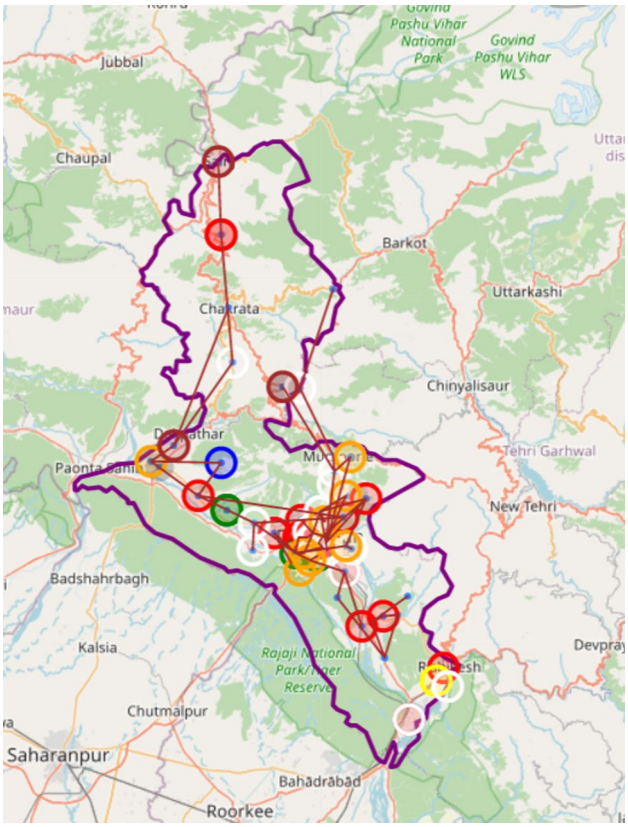

Figure 26. Optimal clustered zones with connecting lines[47], map generated using Leaflet data by openstreetmap wiki.

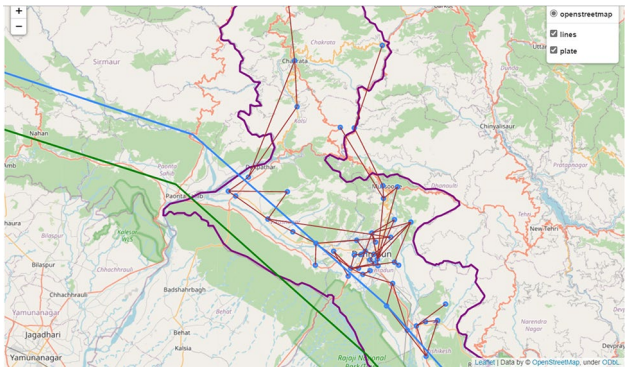

Figure 27. Distribution lines of Dehradun grid with tectonics plates[47], map generated using Leaflet data by openstreetmap wiki.

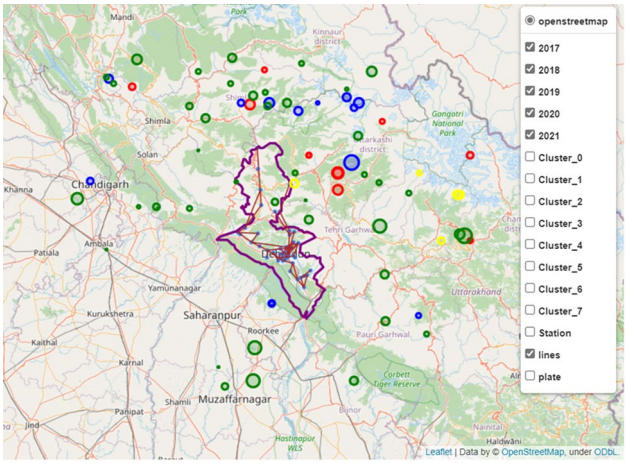

Figure 28. All the station lines and the circles show the previous earthquake points and magnitude[47], map generated using Leaflet data by openstreetmap wiki.

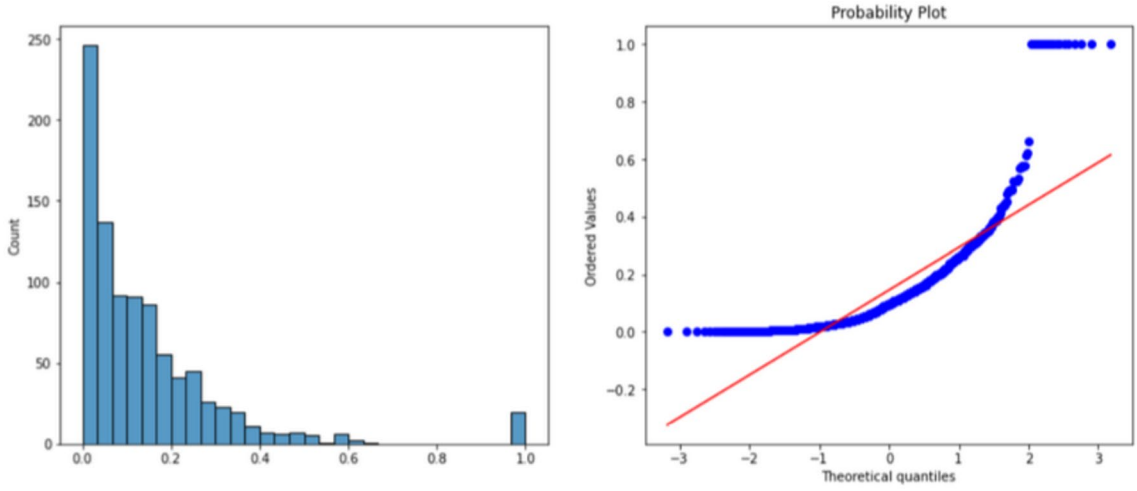

Figure 29. Initial PGA value distribution.

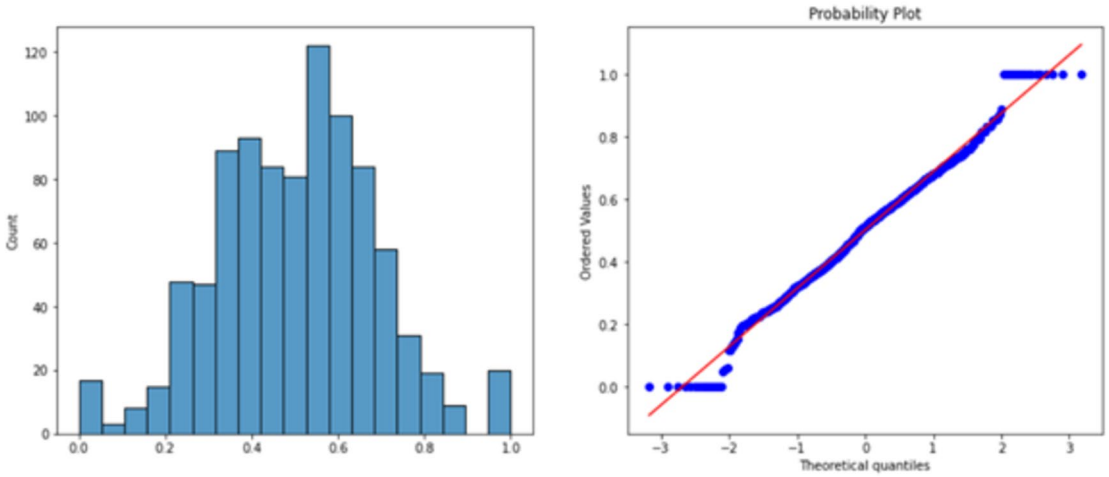

Figure 30. Final data distribution after conversion.

S. no	Damage state impact	Classification range	Practical value obtained
1	High impact	If the values above [mean + 2*(standard deviation)]	Values above 21.279
2	Moderate impact	If the values lie between (mean + standard deviation) and (mean + 2*standard deviation)	Values above 15.3208 and less than 21.279
3	Normal impact	If the values lie between (mean–standard deviation) and (mean + standard deviation)	Values between 9.362 and 15.320
4	Low impact	If the values lie between (mean–2*standard deviation) and (mean—standard deviation)	Values between 9.3620 and 3.403
5	Very low impact	If the values less than [mean–2*(standard deviation)]	Values less than 3.403

Table 4. Damage state classification.

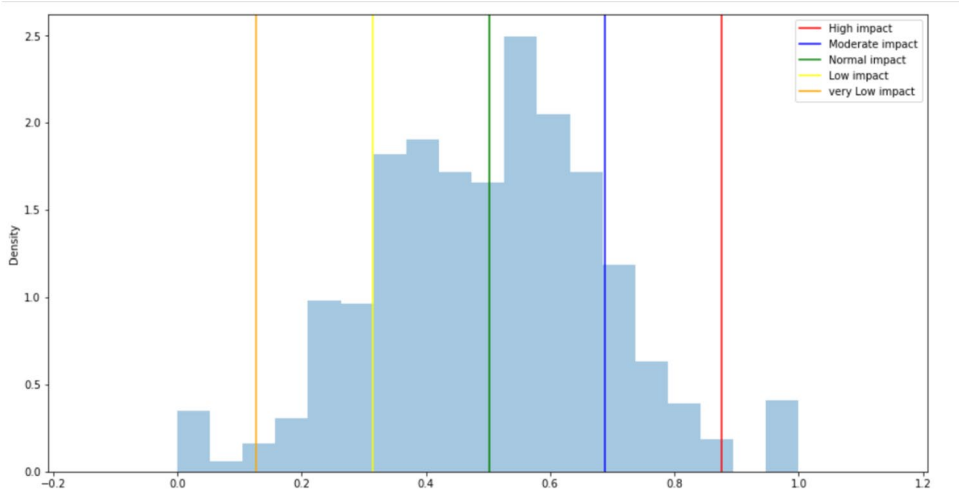

Figure 31. Classifying PGA values into 5 different segments.

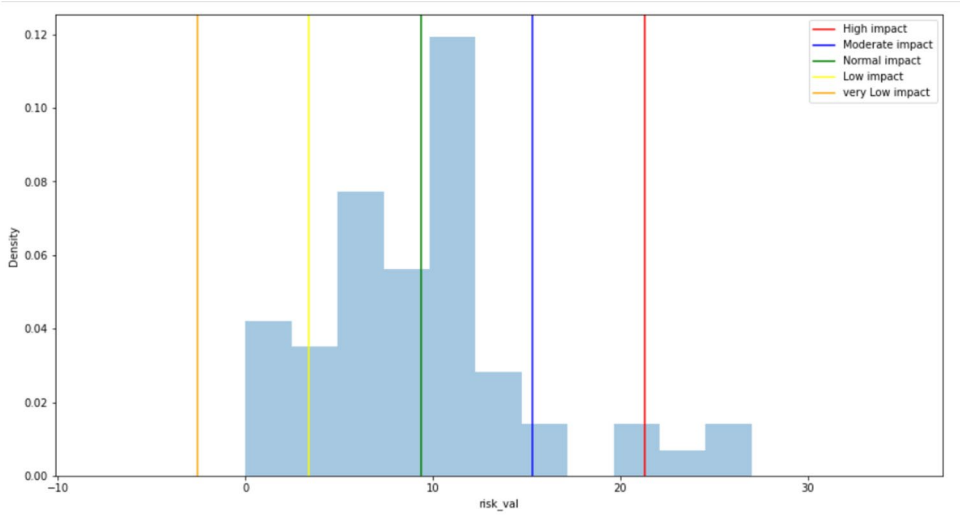

Figure 32. Damage state with respect to practical data.

S.no	Location	Latitude	Longitude	Population	Tourism index	Critical load	risk_val	cluster_label
0	Ajabpur	30.2922	78.0396	24,941	0	0	6	0
1	Anarwala	30.3657	78.0445	399	0	1	11	5
2	Araghar	30.3069	78.0499	1399	1	1	7	5
3	Bairaj	30.0767	78.2896	1507	0	0	0	5
4	Bhaniyawala	30.3657	78.0445	4572	0	1	11	5
5	Bhupatwala	30.8223	77.8546	8763	0	0	4	2
6	Bindal	30.3305	78.0297	7600	0	1	10	2
7	Chakrata road	30.3334	78.0235	3498	0	0	10	5
8	Dakpathar	30.3916	78.0944	17,992	1	1	12	6
9	Dhakrani	30.448	77.7195	12,757	0	0	6	6
10	Doiwala	30.1759	78.1242	8709	0	0	21	2
11	Ganeshpur	30.3026	77.916	2542	0	0	14	5
12	Govindgarh	30.3237	78.0203	8384	0	1	10	2
13	Harbertpur	30.4383	77.736	58,072	0	0	7	3
14	Hathibarkala	30.348	78.0523	13,965	0	0	10	6
15	HimalayanHospital11kV	30.1931	78.165	5878	1	1	4	2
16	ITpark	30.3015	78.0583	6191	1	0	5	2
17	Jhajra	30.3461	77.9182	2923	1	0	24	5
18	Jollygrant11kVI	30.3305	78.0297	9297	1	1	10	2
19	Kargi	30.2849	78.0238	16,412	0	0	6	6
20	Kaulagarh	30.3518	78.0095	9578	0	0	12	2
21	Kyarkuli	30.4327	78.0709	1743	0	0	16	5
22	Lachhiwala11kVI	30.3916	78.0944	1686	0	0	12	5
23	Lakhamanda l11kV	30.3015	78.0583	1044	0	0	5	5
24	Laal Tappad11kVI	30.4555	78.1023	15,038	0	0	27	6
25	Landour11kVII	30.4555	78.1023	3539	1	0	27	5
26	Majra	30.2966	77.9966	21,949	0	0	9	0
27	ManeriBhali	30.267	78.0909	1271	0	0	4	5
28	Miyawala11kVII	30.267	78.0909	8007	0	0	4	2
29	Mohanpur	30.3306	77.9574	8745	0	0	15	2
30	Nagarpalika11kV	30.10647	78.28156	8600	0	0	0	2
31	Nagthat	30.5721	77.9721	47,329	0	0	11	3
32	Nainibagh	30.5705	78.0046	2878	0	0	10	5
33	Natraj	30.3266	78.0357	831	1	1	9	5
34	Niranjanpur	30.2967	78.0141	18,081	0	0	8	6
35	ParadeGround	30.3245	78.0484	8635	1	0	8	2
36	PatelRoad11kVII	30.3136	78.04045	9425	0	0	7	2
37	Purukulgoan	30.4098	78.0675	411	0	0	14	5
38	Raipur	30.5721	77.9721	32,900	0	0	11	7
39	Raiwala11kV	30.0222	78.2147	6558	0	0	0	2
40	RamnagarDanda	30.2967	78.0141	20,619	0	0	8	0
41	Rishikesh	30.0869	78.2676	102,138	1	0	0	4
42	Rudrapur	30.4459	77.8533	140,857	0	0	11	1
43	SIDCUL	30.3572	78.087	7979	0	0	10	2
44	Saharanpur Road	30.31759	78.028984	212	0	0	8	5
45	Sahaspur	30.3927	77.8096	8841	0	0	9	2
46	Sahastradhara	30.387231	78.131606	11,839	1	0	10	2
47	Sahiya	30.6115	77.8753	197	0	0	20	5
48	Savra11kV	30.82238	77.8546	8643	0	0	4	2
49	Selaqui	30.3682	77.8653	22,583	0	0	14	0
50	Selaqui2	30.3682	77.8653	22,583	0	0	14	0
51	Shantikunj	30.309	78.0948	12,889	0	0	6	6
52	SportsCollege	30.3035	78.1046	2878	0	0	5	5
53	TransportNagar	30.022	78.2147	938	0	0	0	5
54	Tyuni	30.9429	77.8496	40,474	0	0	2	7
55	Turner Road	30.26849	78.0069	17,031	0	0	6	6

Continued

S.no	Location	Latitude	Longitude	Population	Tourism index	Critical load	risk_val	cluster_label
56	Vasant Vihar	30.3226	78.0037	11,982	0	0	10	2
57	VikasNagar	30.475	77.7652	40,661	0	0	9	7

Table 5. Cluster zone and associated risk value.

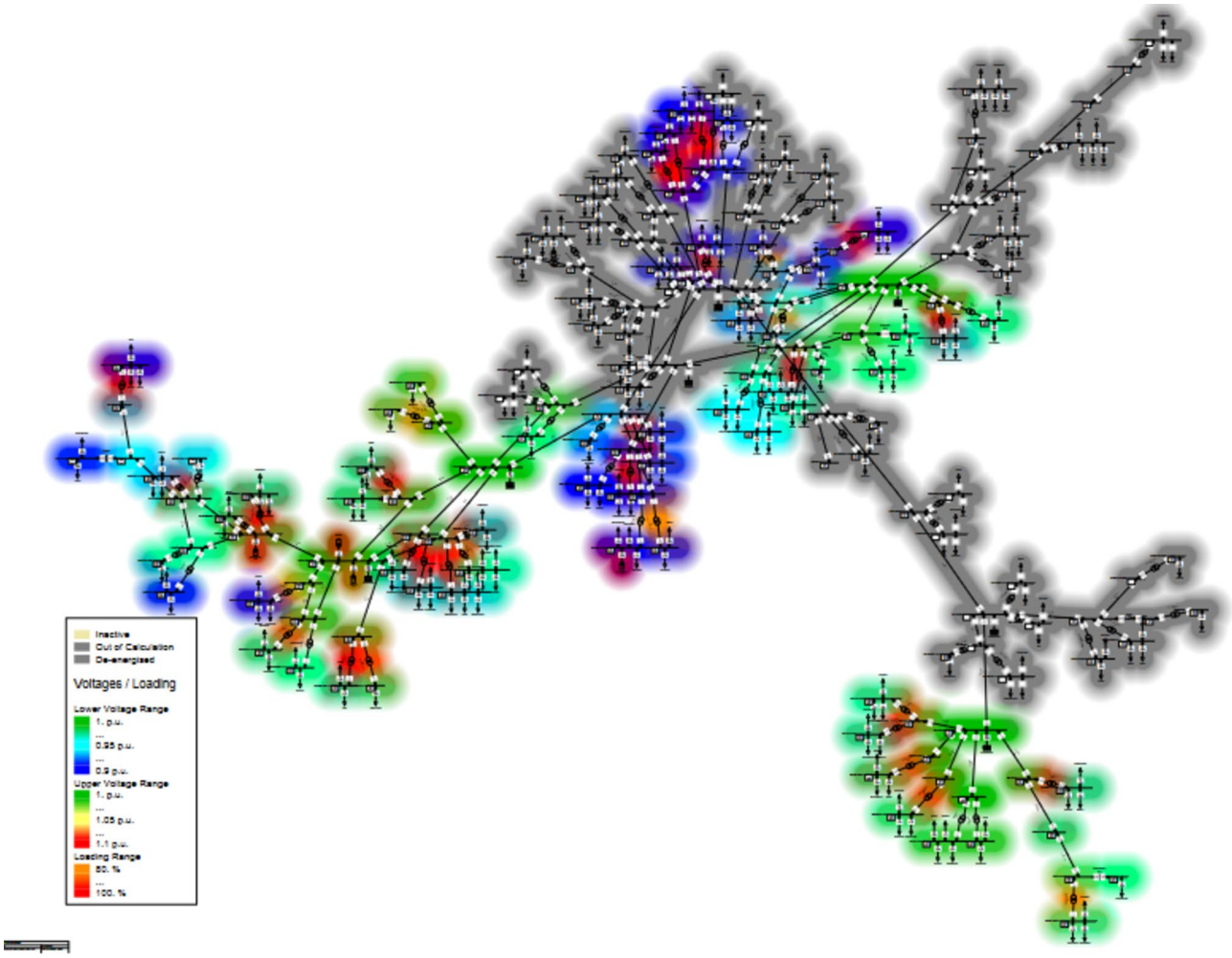

Figure 33. The heat map of study grid after disruption.

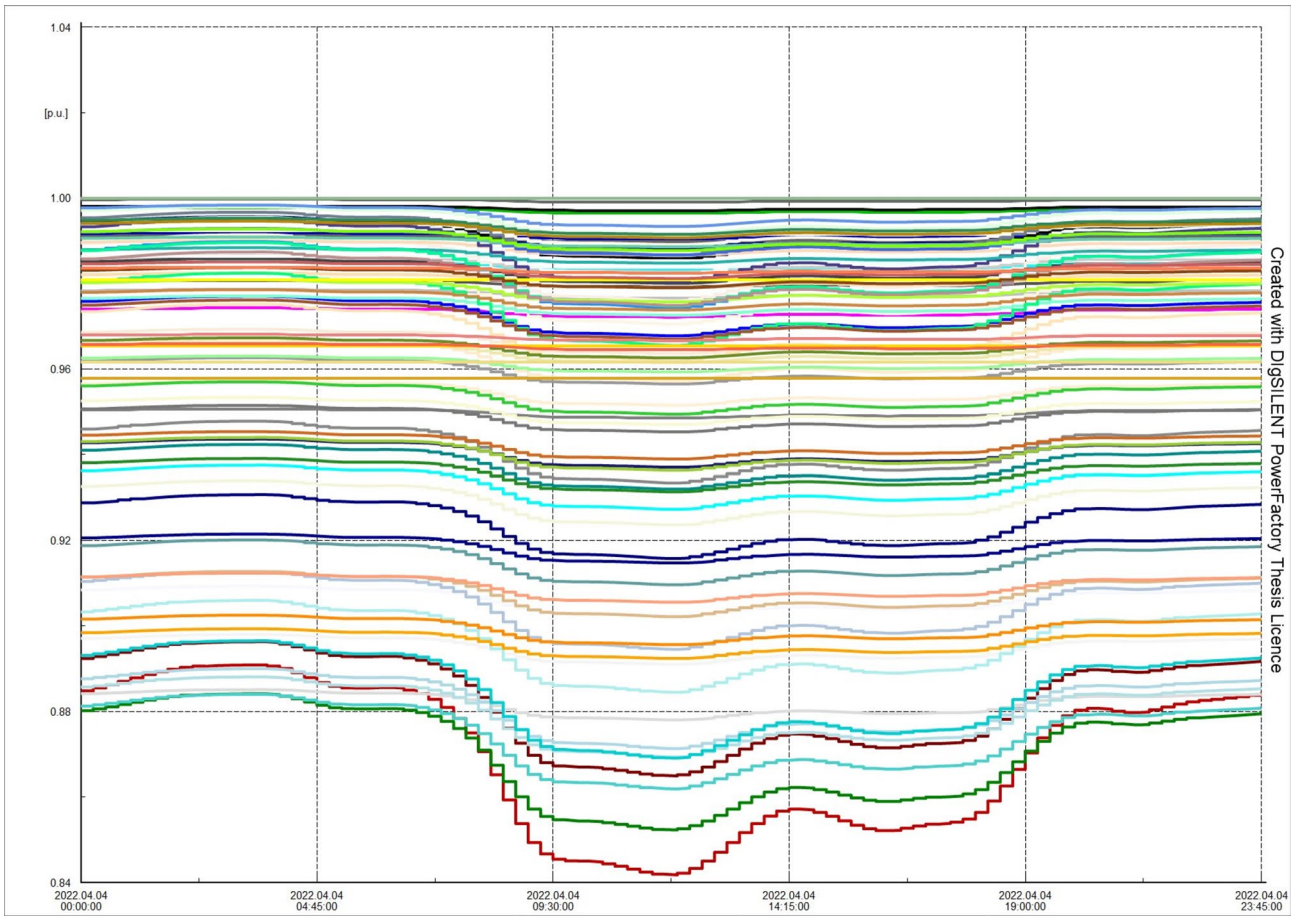

Figure 34. Dehradun Grid profile after natural disruption damage for 24 h.

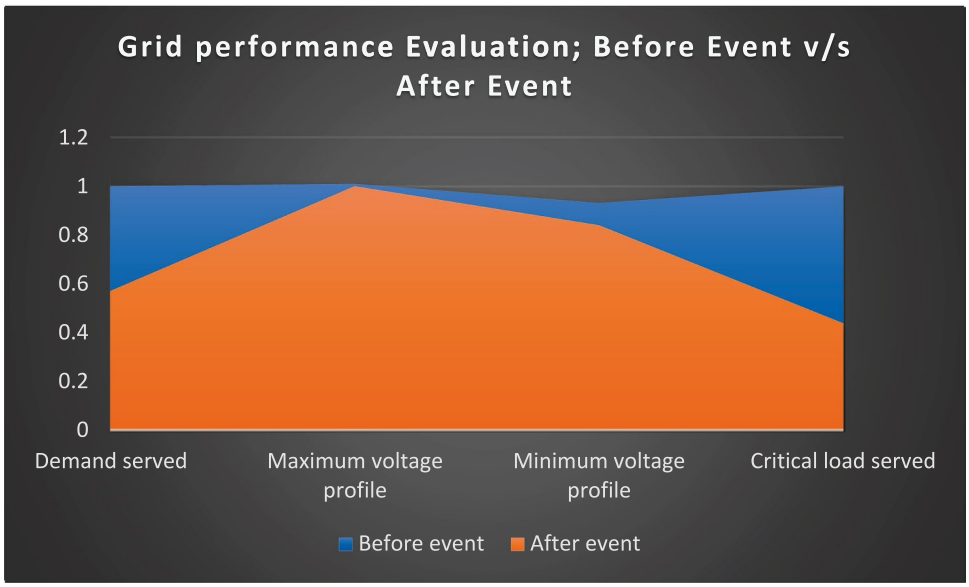

Figure 35. Parametric evaluation of taken grid case; before and after an event.

Data availability

The raw data being used to generate the simulation profile has been provided in the form of Annexure 1–3. To generate the clustering and earthquake profile can be found at the given below link. https://drive.google.com/drive/folders/1hjhM1VAgIcjZlsT0466AdV7y-quRNkQB?usp=drive_link.

Received: 6 August 2023; Accepted: 17 July 2024
Published online: 24 July 2024

References

1. Khalid, M. Smart grids and renewable energy systems: Perspectives and grid integration challenges. *Energy Strategy Rev.* **51**, 101299 (2024).
2. CLP Power Hong Kong Limited, *Smart grid*, https://www.clp.com.hk/en/about-clp.
3. Yadav, M., Pal, N. & Saini, D. K. Microgrid control, storage, and communication strategies to enhance resiliency for survival of critical load. *IEEE Access* **8**, 169047–169069 (2020).
4. Abdel-Hamed, A. M., El-Shafhy, M. M. & Badran, E. A. A new method for ferroresonance suppression in an IEEE 33-bus distribution system integrated with multi distributed generation. *Sci. Rep.* **13**(1), 3381 (2023).
5. Yang, N. C. & Yang, H. Y. Determination strategies of low-voltage ride-through/zero-voltage ride-through curves in Taiwan grid codes. *Electr. Power Syst. Res.* **227**, 109984 (2024).
6. Sharma, A., Kapoor, A. and Chakrabarti, S. Impact of plug-in electric vehicles on power distribution system of major cities of India: A case study. *Dept. Electr. Eng. Indian Inst. Technol. Kanpur, Kanpur, India, Rep* (2019).
7. Mohammed, A. *et al.* Strategies and sustainability in fast charging station deployment for electric vehicles. *Sci. Rep.* **14**, 283 (2024).
8. Dharavat, N. *et al.* Optimal allocation of renewable distributed generators and electric vehicles in a distribution system using the political optimization algorithm. *Energies* **15**(18), 6698 (2022).
9. Yuvaraj, T., Devabalaji, K. R., Thanikanti, S. B., Aljafari, B. & Nwulu, N. Minimizing the electric vehicle charging stations impact in the distribution networks by simultaneous allocation of DG and DSTATCOM with considering uncertainty in load. *Energy Rep.* **10**, 1796–1817 (2023).
10. Behera, M. D. *et al.* Assessment of tropical cyclone amphan affected inundation areas using sentinel-1 satellite data. *Trop. Ecol.* **63**, 9–19 (2022).
11. Ramakrishnan, R. *et al.* Wave induced coastal flooding along the southwest coast of India during tropical cyclone Tauktae. *Sci. Rep.* **12**, 19966 (2022).
12. Mishra, M. *et al.* Geo-ecological, shoreline dynamic, and flooding impacts of Cyclonic Storm Mocha: A geospatial analysis. *Sci. Total Environ.* **917**, 170230 (2024).
13. Biswas, G., Pramanik, S., Bhattacharjee, K. & Saha, S. K. Understanding the response of phytoplankton to the cyclonic event Sitrang: A case study in the Hooghly estuary of Sundarban Bay of Bengal region. *Int. J. Exp. Res. Rev.* **32**, 309–322 (2023).
14. Chakraborty, T., Pattnaik, S. & Joseph, S. Influence of tropical cyclone Jawad on the surface and sub-surface circulation in the Bay of Bengal: Ocean–atmosphere feedback. *Ocean Dyn.* **73**, 619–637 (2023).
15. https://en.wikipedia.org/wiki/Cyclone_Amphan
16. https://en.wikipedia.org/wiki/Cyclone_Tauktae
17. https://en.wikipedia.org/wiki/Cyclone_Mocha
18. https://en.wikipedia.org/wiki/Cyclone_Sitrang
19. https://en.wikipedia.org/wiki/Cyclone_Jawad
20. Yadav, M., Pal, N. & Saini, D. K. Resilient electrical distribution grid planning against seismic waves using distributed energy resources and sectionalizers: An Indian's urban grid case study. *Renew. Energy* **178**, 241–259 (2021).
21. Osman, S. R., Sedhom, B. E. & Kaddah, S. S. Impact of implementing emergency demand response program and tie-line on cyber-physical distribution network resiliency. *Sci. Rep.* **13**(1), 3667 (2023).
22. Extremely Severe Cyclonic Storm MOCHA-A Brief Report_24May2023_with_annexure.pdf.
23. Paul, DK., Singh, Y., Dubey, R.N. Damage to Andaman & Nicobar islands due to earthquake and tsunami of Dec. 26, 2004. In *SET Golden Jubilee Symposium*, 21 (2012).
24. Mohapatra, M., Nayak, D. P., Sharma, R. P. & Bandyopadhyay, B. K. Evaluation of official tropical cyclone track forecast over north Indian Ocean issued by India Meteorological Department. *J. Earth Syst. Sci.* **122**, 589–601 (2013).
25. India raises flood death toll to 5700 as all missing persons now presumed dead, *CBS* (2013).
26. Che, L., Khodayar, M. & Shahidehpour, M. Only connect: Microgrids for distribution system restoration. *IEEE Power Energy Mag.* **12**(1), 70–81 (2013).
27. Yuan, W. *et al.* Robust optimization-based resilient distribution network planning against natural disasters. *IEEE Trans. Smart Grid* **7**(6), 2817–2826 (2016).
28. Korjani, S., Facchini, A., Mureddu, M., Caldarelli, G. & Damiano, A. Optimal positioning of storage systems in microgrids based on complex networks centrality measures. *Sci. Rep.* **8**(1), 16658 (2018).
29. Naderipour, A. *et al.* Spotted hyena optimizer algorithm for capacitor allocation in radial distribution system with distributed generation and microgrid operation considering different load types. *Sci. Rep.* **11**(1), 2728 (2021).
30. Silva, F. F., Carvalho, P. M. & Ferreira, L. A. A quantum computing approach for minimum loss problems in electrical distribution networks. *Sci. Rep.* **13**(1), 10777 (2023).
31. Huang, G., Wang, J., Chen, C. H. E. N., Guo, C. & Zhu, B. System resilience enhancement: Smart grid and beyond. *Front. Eng. Manag.* **4**(3), 271–282 (2017).
32. Umunnakwe, A., Huang, H., Oikonomou, K. & Davis, K. R. Quantitative analysis of power systems resilience: Standardization, categorizations, and challenges. *Renew. Sustain. Energy Rev.* **149**, 11125 (2021).
33. Hatanaka, T., Chopra, N., Ishizaki, T. & Li, N. Passivity-based distributed optimization with communication delays using PI consensus algorithm. *IEEE Trans. Autom. Control* **63**(12), 4421–4428 (2018).
34. Zhou, Y., Panteli, M., Moreno, R. & Mancarella, P. System-level assessment of reliability and resilience provision from microgrids. *Appl. Energy* **230**, 374–392 (2018).
35. Carlson, J.L. et al. Resilience: Theory and application (No. ANL/DIS-12-1). Argonne National Lab (ANL) (2012).
36. Zadsar, M., Haghifam, M. R. & Miri Larimi, S. M. Approach for self-healing resilient operation of active distribution network with microgrid. *IET Gen. Transm. Distrib.* **11**(18), 4633–4643 (2017).
37. Stadler, M. & Naslé, A. Planning and implementation of bankable microgrids. *Electr. J.* **32**(5), 24–29 (2019).
38. Tierney, K. & Bruneau, M. Conceptualizing and measuring resilience: A key to disaster loss reduction. *TR News* **250**, 14–17 (2017).
39. Hou, K. *et al.* A reliability assessment approach for integrated transportation and electrical power systems incorporating electric vehicles. *IEEE Trans. Smart Grid* **9**(1), 88–100 (2019).
40. Dalal, R. & Kumar Saini, D. Mitigation of the impacts of electric vehicle charging on energy star ratings for residential buildings in India. *Clean Energy* **7**(5), 981–993 (2023).

41. Kennedy, J., Eberhart, R. Particle swarm optimization. In *Proc. of ICNN'95-International Conference on Neural Networks*, Vol. 4, 1942–1948 (1995).
42. Nezamabadi-pour, H., Rostami-Shahrbabaki, M. & Maghfoori-Farsangi, M. Binary particle swarm optimization: Challenges and new solutions. *CSI J. Comput. Sci. Eng.* **6**(1), 21–32 (2008).
43. Wadhwa, C.L., Electric power systems. *New Age Int.*, pp 887 (2015).
44. Hassan, A. S., Sun, Y. & Wang, Z. Multi-objective for optimal placement and sizing DG units in reducing loss of power and enhancing voltage profile using BPSO-SLFA. *Energy Rep.* **6**, 1581–1589 (2020).
45. DIgSILENT, Power system solutions, Power Factory 2024. www.digsilent.de.
46. Ye, Q. *et al.* A clustering-based competitive particle swarm optimization with grid ranking for multi-objective optimization problems. *Sci. Rep.* **13**(1), 11754 (2023).
47. https://realpython.com/python-folium-web-maps-from-data/
48. Andreotti, G. & Lai, C. G. Use of fragility curves to assess the seismic vulnerability in the risk analysis of mountain tunnels. *Tunnel. Undergr. Space Technol.* **91**, 103008 (2019).

Author contributions

DKS and MY performed the simulations and wrote the main manuscript text. Data curation has been done by DKS. NP has supervised the work. All authors reviewed the manuscript.

Competing interests

The authors declare no competing interests.

Additional information

Supplementary Information The online version contains supplementary material available at https://doi.org/10.1038/s41598-024-67927-5.

Correspondence and requests for materials should be addressed to D.K.S. or M.Y.

Reprints and permissions information is available at www.nature.com/reprints.

Publisher's note Springer Nature remains neutral with regard to jurisdictional claims in published maps and institutional affiliations.